A system for the ammonolysis of oxy-sulfide glasses

by

Peter Anthony Enz

A thesis submitted to the graduate faculty

in partial fulfillment of the requirements for the degree of

MASTER OF SCIENCE

Major: Materials Science and Engineering

Program of Study Committee:
Dr. Steve W. Martin, Major Professor
Dr. Michael Bartlett
Dr. Aaron Rossini

The student author and the program of study committee are solely responsible for the content of this thesis. The Graduate College will ensure this thesis is globally accessible and will not permit alterations after a degree is conferred.

Iowa State University

Ames, Iowa

2017

DEDICATION

To my parents Mary and Richard Enz

TABLE OF CONTENTS

LIST OF FIGURES

Page

LIST OF TABLES

NOMENCLATURE

BOs	Bridging Oxygens
BSs	Bridging Sulfurs
DSC	Differential Scanning Calorimetry
DTA	Differential Thermal Analysis
EH&S	Environmental Health and Safety
FPM	Facilities Planning and Management
NBOs	Non-bridging Oxygens
NBSs	Non-bridging Sulfurs
Tc	Crystallization Temperature
Tg	Glass Transition Temperature
XPS	X-Ray Photoelectron Spectroscopy
XRD	X-Ray Diffraction

ACKNOWLEDGMENTS

I would like to thank my committee chair, Dr. Steve W. Martin, and my committee members, Dr. Michael Bartlett, and Dr. Aaron Rossini, for their guidance and support throughout the course of this research.

In addition, I would also like to thank my friends, the GOM group, the MSE department faculty and staff for their help in my time at Iowa State University. I would like to specifically thank both FPM and EH&S here at Iowa State University for their help in setting up the ammonolysis system in knowing the required regulations and the realization properly following those regulations. Of particular help at EH&S was Ashley Chargualaf in the process of setting up the ammonolysis system and developing standard operating procedures that adhere to safety requirements. I would like to thank the ISU Materials Analysis and Research Laboratory (MARL) and Dapeng Jing for assistance in running XPS on the nitrided samples.

I wish to thank Dr. Steven Veysey Director of the ISU Chemical Instrumentation Facility for training and assistance pertaining to the PE 2100 CHN/S elemental analysis results included in this work. Purchase of the Perkin Elmer 2100 Series II CHN/S analyzer used to obtain results included in this publication was supported in part by the National Science Foundation under Grant No. DBI 9413969. Any opinions, findings, and conclusions or recommendations expressed in this material are those of the author and do not necessarily reflect the views of the National Science Foundation.

This research was supported by a grant from the Honda of America Corporation, the National Science Foundation under grant number DMR1304977, by the Department

of Energy under contract number DE-AR0000778, and by the Department of Materials Science and Engineering, the College of Engineering and the Graduate College at Iowa State University of Science and Technology. This support of this research is gratefully acknowledged.

ABSTRACT

Solid electrolytes for batteries are of particular interest for future green technology use. Oxy-sulfide glasses are some of the most conductive glassy ion conductors and are explored here for their potential in incorporation of nitrogen by ammonolysis. In an attempt to stabilize the volatile sulfide glass and further increase conductivity, a system for the ammonolysis of oxide and oxy-sulfide glasses has been built and tested for synthesizing lithium ion conducting amorphous materials. Pure oxide, lithium metaphosphate glasses were nitrided with the ammonolysis system, then analyzed and determined to successfully incorporate nitrogen, only more slowly than previous studies. Lithium oxy-sulfide glasses were then nitrided uncovering difficulties in incorporating nitrogen and crystallization upon cooling during ammonolysis.

Techniques to determine how well nitrogen was incorporated into the glass were combustion and XPS, while the structure was analyzed with IR and Raman spectroscopy, the glass transition temperature was determined with DSC, and ionic conductivity was determined through electrochemical impedance spectroscopy. Both nitridation parameters and glass properties were investigated to identify potential issues with the system, with flow rate, gas flow, glass composition, crystallization and internal bubbles being primary issues that will need to be overcome to successfully nitride oxy-sulfide glasses.

CHAPTER 1. INTRODUCTION

Of current great interest are new renewable energies to enable a green sustainable future on our planet. Many of these energy technologies generate an intermittent supply of energy depending on the sun and wind [2]. This creates a need for storage technologies to supply this energy at all times and make it mobile, providing a need for battery technology advancements. One of the most promising areas for advancements in battery technology is the use of solid electrolytes to allow for greater capacity using pure lithium and sodium anodes and thereby replacing permeable and flammable electrolyte materials that lead to shorting and fires [3, 4].

One type of solid electrolyte being explored are fast ion-conducting glassy materials, however, they have some of their own new issues [5]. A glass material is already envisioned to have the first need for an electrolyte material in that it is a dielectric and an insulator of electronic current. A primary interest in solid glassy electrolytes is their potential to enable the use of more energy dense anode and cathode materials. Significant gains in anode specific capacity over conventional LiC_6 intercalation with 372 mAh/g capacity nearing an order of magnitude and approaching 4000 mAh/g for pure lithium and lithium alloys [3, 4]. The intent is to use a solid glassy electrolyte preventing shorting from a dendrite growing through the electrolyte [5]. The glass material in an electrolyte needs to be robust enough to withstand the forces experienced from the transport of lithium between cathode and anode sides of the battery which in some cases result in changes in volume. An advantage over other solid electrolytes that glassy solid electrolytes have is that they have no grain boundaries in which dendrites can grow along

[6, 7]. With high fracture strength glasses it may be possible to prevent shorting from dendrite growth through the electrolyte. The challenge of a solid glassy electrolyte that must be addressed is maintaining the strength and electrical insulating properties, while increasing the ionic conductivity of the glass to a level on par with existing liquid electrolytes. Chalcogenide glasses have become an area of intense research in ion conducting materials.

The first ion conducting glasses were modified oxide glasses with high alkali modifier content in the glass [8]. These further gains in conductivities were achieved by opening up and breaking up the glass network with glass additives that add more of the conductive ion to the glass [8]. Addition of halide salts such as LiI to the glass creates conductive pathways in the glass but again weaken the glass by breaking up its network [9, 10]. A change to the glass formers in the glass that can change the properties of the glass including the ionic conductivity is the Mixed Glass Former Effect (MGFE) [11-14]. In this effect, two or more different glass formers are combined and can create a boost or reduction from a linear change in properties, which can result in a boosts in ionic conductivity.

The current best fast ion conducting glasses are sulfide glasses that have conductivities commonly between 10^{-3} to-10^{-2} S/cm^2 for lithium glasses, which is approaching the desired conductivity but are relatively unstable [15-18]. Since the early 1980s, sulfide glasses have been of interest due to their higher ionic conductivity which arises from larger more polarizable sulfur anions relative to oxygen [19]. This enables a higher alkali ion conductivity since the coulombic attraction of the between the anion and cations is smaller and the larger atomic radii of the sulfide anion compared to the oxide

anion creates larger interstitial openings for the ions to conduct through [19, 20]. Sulfide fast ion conducting glasses have a number of drawbacks that must be overcome to achieve viability in batteries. Some of these include their weak mechanical strength, low glass transition temperature and thermal stability, decomposition in air and water, and finally further improving their ionic conductivity [6, 21].

Researchers have discovered the addition of small amounts of oxide glass former back into pure sulfide glasses can lead to a further increase in ionic conductivity [22, 23]. Typically, adding ca. 10 mol% oxide glass former can lead to as much as an additional order of magnitude of conductivity gain [23]. Beyond the first 10 mol% of oxide glass former the conductivity tails off below that of the base sulfide glass. In addition to the ionic conductivity gains oxy-sulfides glasses are more stable in air, than sulfide glasses, however still more chemically unstable than pure oxide glasses.

The remaining problems of the oxy-sulfide glasses can potentially be addressed by incorporation of nitrogen in their glass network as has previously been done by a number of groups with numerous oxide glasses [24-49]. Water soluble alkali phosphate glasses were made more robust in the 1980s by ammonolysis, in both the Marchand and Day research groups, showing an increase in Tg, decrease in water solubility, and an increase in hardness due to the greater networking imparted by the nitrogen molecular crosslinking [25, 27, 30, 33, 50]. In addition to addressing the stability concerns still present in oxy-sulfide electrolyte materials, the potential is seen in nitrided phosphate glasses to have a increase in conductivity and electrochemical stability [46, 48, 49]. Oxy-nitride lithium phosphate thin film glasses made by the Dudney group in the 1990s found

the incorporation of nitrogen to enable electrochemically stable contact of the electrolyte film to lithium metal [49].

A variety of techniques can be used to nitride glasses including high temperature melts, and high temperature and pressurized nitride melts, sol gels with nitrides, and ammonolysis (running ammonia gas over glass) at relatively lower temperatures [32, 33, 36, 39, 40, 43-52]. An ammonolysis system was chosen in this work due to its low temperature nature, ease of use, and desire to use with sulfide glasses. Previously, groups including Marchand, Day, and Muñoz have used ammonolysis to nitride alkali phosphate melts resulting in increases in glass transition temperature, decrease in dissolution rate in water, and an increase in ionic conductivity [24, 27, 30, 33, 36, 39]. The only previous synthesized nitrided sulfide glass was a two-step process by Muñoz and Tatsumisago of mechanically milling an oxide glass from ammonolysis with a sulfide glass or a purely mechanically milling process with sulfides and lithium nitride [37, 53-55]. In this work, sulfide glasses will be explored as base glasses for ammonolysis without nitriding an oxide, in a single nitridation step as a bulk glass.

To achieve the goal of nitrided oxy-sulfide glasses that would still be conductive but stable in air, an ammonolysis system for the incorporation of nitrogen was assembled. The system was run to optimize and prove its viability for nitriding of sulfide glasses in a single step process. Once the system was built, compositions of base glass samples were transferred to the atmosphere purged with nitrogen and then run with ammonia flow for an intended experiment duration. Variables adjusted include starting glass composition, gas flow rate, ammonolysis temperature, and cooling conditions. These experiments allowed for inferences into the viability of such a system for use with sulfide glasses and

the basic understanding of how nitrogen incorporates by using proved lithium meta-phosphate glasses similar to work by Muñoz et. al. [34, 36, 37, 39, 40, 42, 53, 56-58]. The results of this work show some differences and learning points such as the best way in our work to accurately measure nitrogen content in the glasses to be XPS and how to successfully load and unload the furnace.

New sulfide based glass compositions were prepared and nitrided in the ammonolysis system to more achieve the goal of a glass with the advantages of both a conductive sulfide and a nitrided glass. A variety of outcomes occurred from nitriding these glasses, such as bubbles, weight losses, crystallization, and compositional changes including an increase in glass transition temperature. Compositions that did not cool into glasses in the furnace led to analysis of the crystalline and semi-crystalline products to understand the phases present using IR and Raman spectroscopies with the potential for future XRD analysis. The results show both potential to achieve the ammonolysis goals but leaves a number of challenges in achieving glassy nitrided samples that are not crystalline or with large weight losses.

CHAPTER 2. BACKGROUND AND OBJECTIVES OF THESIS

A. Nitridation of Glass Forming Liquids

i. Ways nitrogen is introduced and why ammonolysis is used with sulfides

The incorporation of nitrogen in a glass network has been used as a means to improve the properties of glass for several decades in a number of applications, but as of yet has been unexplored as a single step process for sulfide glasses except for mechanical milling [37, 54, 59, 60]. There are several ways nitrogen can be intimately incorporated into a glass network, these are high pressure and temperature glass melts with nitrides added as the nitrogen source, sol gel processes, sputtering of glass in a nitrogen atmosphere and ammonolysis of glass melts [33, 43, 45, 46]. The first three techniques are not used in this work due to their poor ability to be scaled up or poor compatibility with sulfide synthesis.

a. High temperature and pressure nitride melts

High temperature synthesis of nitride glass melts is the first method of nitriding glasses and was primarily silicate related SiON and SiAlON glasses. Initially, the interest in these glasses arose from understanding their occurrence in SiAlON or silicon nitride ceramic grain boundaries, before becoming of interest for their own properties such as their elastic moduli, glass transition temperature (thermal stability), viscosity, thermal expansion coefficient, hardness, and weight [61, 62]. The glasses are often referred to as MSiAlONs, where the M can refer to a modifier cation that can be an alkali, alkaline earth, or lanthanide element, and can be used to tailor the base non-nitrided glass compositions

These syntheses require temperatures between 1500-1700°C, low oxygen partial pressures to avoid glass oxidation, specialized crucible materials and working from a limited number of nitride nitrogen sources [44, 45]. Typically in a melt synthesis, nitrogen is introduced in one of a number of ways, which include bubbling ammonia or nitrogen through the silicate melt or the introduction of nitride compounds into the melt. Later in the 1990s to enable a greater compositional range of synthesis to counter the oxidizing effects of the components of the oxide nitride glass melts, high pressure was incorporated into the synthesis of these oxy-nitride glasses [52].

The use for this type of nitridation for tailoring optical properties, hardness and thermal expansion for applications today is enabled by the replacement of oxygen anions an O^{2-} with a N^{3-} charge resulting in a more networked silicate glass network. In these glasses, elements have several purposes in the network, as mentioned before there are modifiers such as alkalis (Li, Na), intermediates with charges greater than one (Al, Mg, Ca), similar rare earths with charges greater than one (Y, La), and network formers which in this case are silicon [61]. The addition of nitrogen changes the charge balance of as a sort of additional intermediate acting anion oxygen that can have 3 fold rather than 2 fold bonding. Some examples of the effects of the addition of nitrogen tightening the glass network in SiAlON related high temperature nitride melt synthesis are increases in T_gs (thermal properties), molar volume (density), hardness, and Young's modulus [44, 45, 61, 62]. Work by Loehman , demonstrated the effect of nitrogen on glass transition temperature, hardness, and fracture toughness increase with successive nitrogen networking, while thermal expansion values decrease on a nitrided Y-Si-Al-O-N system [45].

b. Sol-gel nitrided glasses

Sol-gel made glasses are synthesized by creating a solution with the desired glass formers and bridging oxygens in organic solvent. The solution is then made into gel and dried by evaporation under air or supercritical conditions [51, 63, 64]. After this the dried gel is run through an ammonolysis furnace below T_g then sintered above its T_g for synthesis of a porous nitrided glass if a nitride was not part of the starting solution [43, 65]. These glasses can open up the synthesis range at relatively low temperature, but more difficult to make with higher conductivity sulfide glasses of interest due to their air sensitivity.

This technique has enabled the study of additional nitrided poor glassforming compositions by extending the glassforming range by not being reliant on the melt formation kinetics and thermodynamics. At high temperatures where oxidation and vaporization can occur, resulting glasses can be dark or gray glasses due to metallic inclusions from the melt [43, 51]. An example of the increased glass formability using the sol-gel ammonolysis is 1980s work by Brinker et al. enabling the synthesis of nitrided M-B-O-N glasses creating glasses containing Si-Al-B-Ba-Na-N which showed Si-O-B sites attacked by the ammonolysis, which otherwise were unable to be synthesized [43].

c. Sputter synthesis of nitrided films

Phosphate glasses were sputtered to create nitrided lithium phosphate glasses (LiPON), first for their ionic conductivity as thin film electrolytes [46, 47, 49]. Here lithium oxide and oxide glass former (phosphorus oxide, silicon oxide, or boron oxide)

target is RF- magnetron sputtered under a nitrogen atmosphere [46, 47, 49]. Using this technique a disordered amorphous product can be synthesized on the micron thickness scale resulting in relatively ionically conductive electrolyte materials producing conductivities acceptable for thin film batteries.

LiPON films synthesized had conductivities greater than 10^{-6} S/cm^2 at room temperature showing favorable stability in contact with solid lithium metal which is beneficial for high energy density lithium thin film batteries and preventing dendrite growth [49]. Additional work Kim et al. on lithium borate targets shows similar 10^{-6} S/cm range conductivity and slightly better cycling thought to be from boron having a single valence state [66]. More recently other targets including boron, germanium, silicon, and sulfur have been explored, but all are limited by either the low yields of thin film synthesis or being less conductive oxide electrolytes [46, 66, 67].

d. Bulk glass ammonolysis

Of interest for sulfide melts as a one-step nitridation process is the addition of nitrogen through ammonolysis, the running of ammonia gas over a melt at high temperature. The technique of ammonolysis of oxide glasses is described by Marchand in Equation 1 as a generalized formula where ammonia and oxygen are replaced nitrogen anions and water, where the limit to the glassforming range was approximately $XPO_2N_{0.67}$ (X representing alkali) [33, 50].This technique has been used on pure alkali phosphate glasses to form bulk rather than thin film glasses.

$$3O^{2-} + 2NH_3 \rightarrow 2N^{3-} + 3H_2O \quad (1)$$

A number of groups have used this method of ammonolysis, first groups related to Marchand and Day researching nitrided phosphate glasses for their thermal, mechanical strength, and increased water resistance properties (durability) [24-30, 33, 50]. These groups found the uptake of nitrogen to be fast and linear for the first 10-12 hours before tailing off at a point where a critical number oxygens are replaced in the glass network [27, 30]. The dissolution rate of the alkali glasses in water, upon nitridation is highly reduced and the effect is greatest the smaller the alkali ion is. The Day group has found when a N/P ratio of 0.4 is achieved in a LiPON or NaPON glass a dissolution rate 1000 times lower is observed demonstrating the large effect nitrogen has on these glasses durability [29]. An increase in glass transition temperature is seen in a nitrided $LiPO_3$ glass that has achieved 2.71 wt. % nitrogen to increase from 325 to 355°C due to the greater nitrogen crosslinking tightening and strengthening the glass [27].

Later, the use of similar phosphate compositions by the Dudney group as thin films led to work by the Munoz and Le Sauze groups who investigated the ammonolysis of alkali phosphates to make potential ion conductors for electrolytes [32, 34, 36, 38-40, 48, 58, 60, 68-70]. These groups were inspired to do this work to build bulk batteries rather than the thin film LiPON batteries that were previously researched. Munoz showed activation energies of nitrided $LiPO_3$ resulted in activation energy reductions from 73.3 kJ mol^{-1} to 66.6 kJ mol^{-1} with 3.6 wt. % nitrogen incorporation, where the conductivity was gained quickly with the first additions of nitrogen [39].

The favorable conductivity of these nitrided alkali phosphate glasses arises from the trivalent and divalent nitrogen atoms replacing oxygen in the glass network as seen in Figure 1[28]. A theory for the increase in conductivity is that the ratio N_t/N_d (triple coordinated to double coordinated nitrogens) affects directly the ratio of BO/NBOs exchanged as seen in Equations 2 and 3 [36]. A resulting replacement of more bridging oxygens leads to a greater ratio of NBOs where lithium ions can conduct through the glass network.

$$N_t = \frac{3}{2} BO \tag{2}$$

$$N_d = 1\, NBO + \frac{1}{2} BO \tag{3}$$

The previous ammonolysis work with ion conductors focused on oxide glasses except for one instance of planetary milling a nitrided oxide with a sulfide glass which leads to our current interest in applying this technique to sulfides and describing the background of these glasses [37, 38].

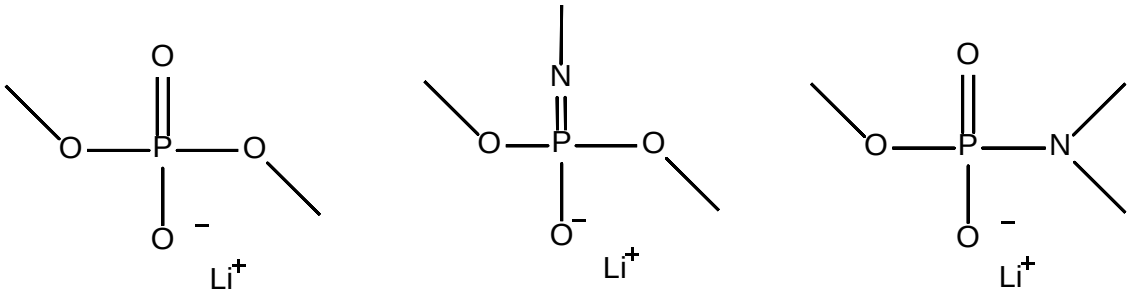

Figure 1- Examples of the repeating unit of lithium metaphosphate unit, along with divalent and trivalent nitrogen substitution in this repeating glass unit. Adapted from M.R. Reidmeyer and D.E. Day [28].

B. Ionic Conduction in Glass

A primary reason for interest in sulfide glasses is their superior ionic conductivity over analogous oxide glasses [19]. The process of ion conduction is explained by a thermally activated process with temperature increasing the number of free ions and mobility of the free ions [12, 71, 72]. In Equation 4, the term n is the number of mobile ions and μ is the mobility of the ions and each have an Arrhenius relationship with temperature with their own separate activation energy terms [71].

$$\sigma_{d.c.}(T) = n(T)eZ\mu(T) \tag{4}$$

The Anderson-Stuart Model depicts the conduction of ions through a glass network and contain two primary components to the activation energy [71]. The two components to the activation energy of ionic conduction are the coulombic binding energy and the strain energy which form the Arrhenius relationship of the conductivity of the ions [71, 72]. The coulombic binding energy arises from the energy required for alkali cation to dissociate from a NBS or NBO anion. The strain energy component is the elastic energy required to dilate the openings between NBO or NBS equilibrium sites in the glass network to allow enough space to allow the conducting ion through [12, 20, 72]. This model is visualized in Figure 2 which depicts an adaptation of the Anderson-Stuart Model by Martin et al. displaying a visualization of the energy barriers that must be overcome for the ion to conduct [13, 72]. The most conductive oxide glasses are those that are highly broken up with a large number of non-bridging oxygens to serve as ions sites and conduction pathways for ions. At the same time the more NBOs the glass has,

the more ionically conductive it becomes. However, the glass becomes less stable because there are fewer BOs holding together the glass network leading to the need for more stable glass ion conductors including nitridation.

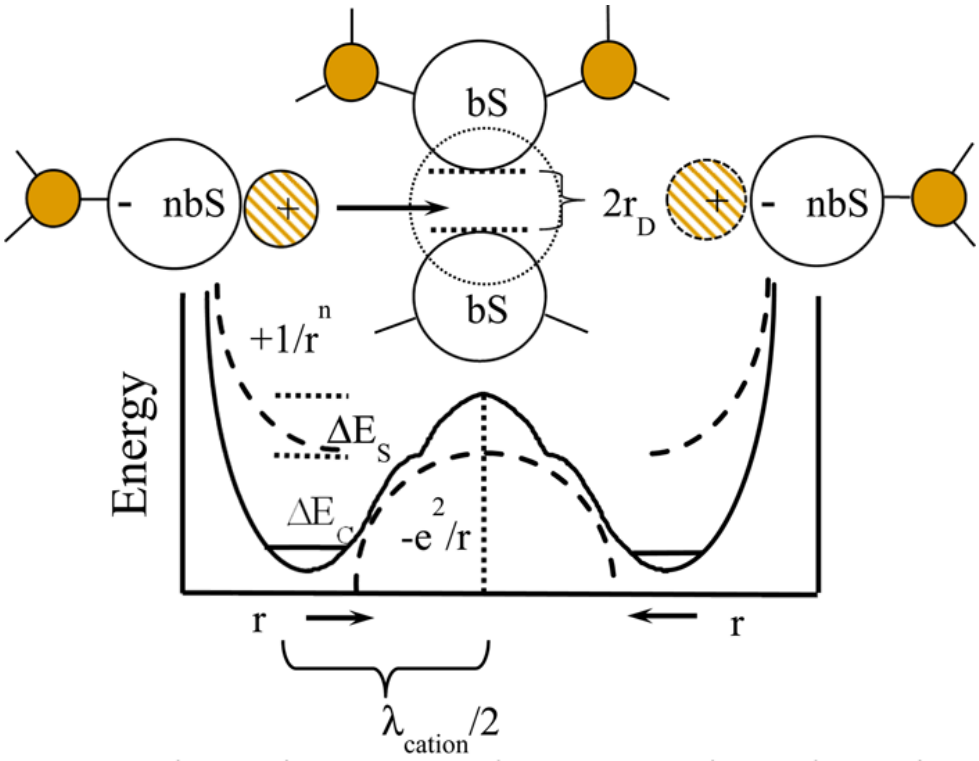

Figure 2 – Reproduction of depiction of Anderson-Stuart Model by Martin showing strain and coulombic energies of ions moving through glass network ion conduction pathway [72].

i. Ionically conducting sulfide glasses

Sulfides glasses are advantageous over oxide glasses due to greater polarizability of the sulfur atom compared to that of oxygen allowing for lithium ions to more easily dissociate from NBSs, and occurs from having a larger electron cloud and being below oxygen in the periodic table [19]. French groups in the late 1970s and early 1980s first researched sulfide glasses for their ionic conductivity properties as means to primarily

improve the ion mobility by changing the composition of the glass network [9, 10, 19]. Replacement of oxygen ions with sulfur ions reduces both coulombic binding energy and volumetric strain terms in the Anderson-Stuart Model to be smaller. The coulombic binding energy term is smaller due to the larger sulfur atom radius making the 1/r term of the coulombic binding energy much smaller and the greater polarizability of sulfur atoms leads to a higher dielectric permittivity. The permittivity has an inverse to the coulombic binding energy [20]. The strain term is smaller in sulfides relative to oxides because of weaker bonding and less dense atomic packing due to larger sulfur atoms creating openings in the glass network [19, 20]. This results in sulfide glasses having orders of magnitude higher ionic conductivities relative to oxide glasses.

Historically, a large number of sulfide glass formers have been explored, but in this work the main glass formers that will be explored are boron, phosphorus, and silicon due to their relative affordability and ionically conductive properties [73]. Each have different ease of use as sulfide materials. Boron sulfide is difficult to make in the lab, silicon sulfide is easily made in the lab, and phosphorus sulfide is commercially available at desired purity [74]. All glass formers can make highly conductive alkali glasses, but each have drawbacks of glassforming range, thermal stability, and methods of synthesis.

ii. Ionically conductive oxy-sulfide glasses

A strategy that has been used to improve the air stability to glasses and to increase the ionic conductivity of sulfide glasses is the replacement of a small amount of sulfide ions with a small amount of oxide ions [22, 75]. It is believed this boost in conductivity is due to the structure having BOs and NBSs in its glass network [22]. This assumes that

the alkali ion sites at the non-bridging sites are preferentially sulfur atoms that are more conductive due to their smaller potential well due to their more malleable electron cloud in non-bridging sites as described in the Anderson-Stuart Model [71, 72].

iii. Drawbacks to sulfide glasses

Sulfide glasses are all prepared in gloveboxes due to their hydroscopic nature that results in the glasses reacting with water and oxygen to form a hydrolyzed soft material expelling hydrogen sulfide gas rather than a solid glass [21]. This leads to a more difficult material to work with from its need to be handled and made primarily in an inert atmosphere resulting in more difficult synthesis, and analysis of the glasses arising from the degradation of the glass when exposed to atmosphere. Starting materials must often be synthesized in silica ampoules for purity and even when making glasses in a glovebox, crucibles and other materials are attacked by the sulfur vapors.

Not only are sulfides volatile in air, but have a number of other drawbacks. These poor properties include their already mentioned poor chemical stability (volatility in both air and as a melt), low mechanical strength, and poor thermal stability (low glass transition temperatures common in high modifier glasses) [6, 21, 76]. Existing nitridation of alkali oxide glasses has been used as a means of addressing these shortcomings in oxide glasses including tuning their optical properties and improving their ionic conductivity.

C. Objectives of Thesis

The objectives of this thesis are to design and build a new system for the ammonolysis of sulfide glasses, including the steps taken to build it and prove the successful incorporation of nitrogen. Currently, oxide glasses are the only glasses that have been nitrided in a single step and this work will describe the initial sulfide results from a variety of alkali-sulfide glass compositions. The next objectives were to investigate properties of the nitrided glasses to explain the potential issues with nitriding sulfide glasses through a variety of analyses. Combustion analysis and XPS were used to analyze the nitrogen contents. The structural changes were analyzed using both IR and Raman for glasses, and XRD for crystalline nitrided products. Thermal properties were investigated using a combination of DSC and DTA depending on temperature ranges of interest. Ionic conductivity was analyzed by impedance spectroscopy of nitrided glasses.

CHAPTER 3. EXPERIMENTAL METHODS

A. Design and Construction of an Ammonolysis System

The first step in nitriding new sulfide glass compositions was building an apparatus for ammonolysis. First, a tube furnace with water-cooled capped furnace ends, and proper ways to introduce nitrogen and ammonia gases in a safe manner were identified. Due to using 99.99% pure ammonia Iowa State University's EH&S department was contacted to determine the correct procedures for setting up a system that uses such a corrosive and volatile gas. This led to several new concerns first finding a controlled room and a proper way to ventilate the ammonia upon an emergency in accordance with EH&S regulations. This resulted in finding a room with access to a fume hood that was controlled (had a locked door), incorporating a ventilated cabinet for the ammonia system into the design, had space for the nitriding system in the department, and writing a standard operating procedure for the operation of the system that involved checking for leaks in the gas lines.

Next, an existing tube furnace was approved for use in the MSE department that was suitable to use with a silica tube with stainless steel water cooled furnace ends in an arrangement as shown in Figure 3. Upon first testing at elevated temperature it was found that a silica furnace tube was not durable enough to withstand the thermal expansion pressures exerted by the steel furnace ends. This led to replacing with a thicker more durable Mullite tube to overcome this issue with the water-cooled steel ends to the furnace and their expansion. Valves were added to the house water line and reinforced Tygon water lines were run to the furnace ends to cool them and minimize their

expansion during operation. Due to the corrosive nature of the ammonia gas, the plumbing and valves on the inlet side of the system were made of either reinforced Tygon or stainless steel. This inlet system as seen in Figure 4 has supply lines that go into flow meters one for each gas that are each followed by a valve. After this the two gas lines tee together and flow to the furnace tube inlet through the Mullite tube and out the furnace outlet where the tube exausts into a ventilation shaft connected to the room's fume hood. Finally 99.99 % purity ammonia and an industrial grade nitrogen cylinder were connected to their respective gas lines.

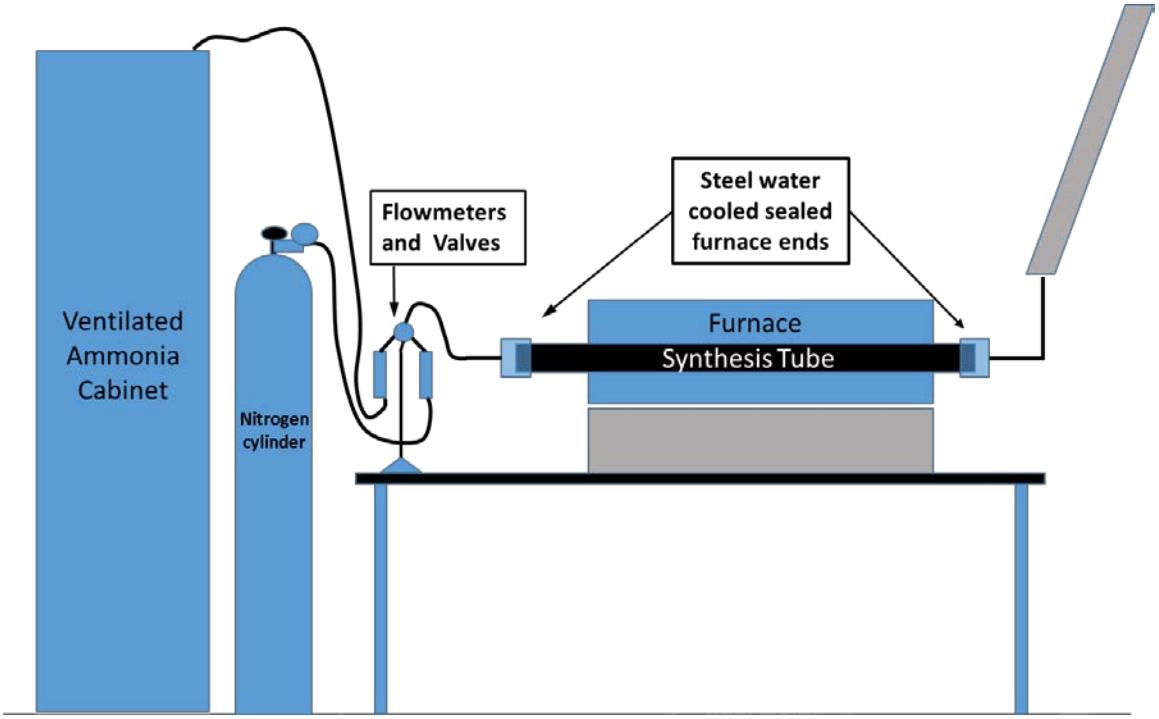

Figure 3 – Diagram of ammonolysis system including measurements of mullite furnace tube, inlet valves, outlet to fume hood exhaust, and the gas cylinders.

Figure 4 – Furnace setup as built in lab.

B. Synthesis of Base Glasses

i. Oxide glass synthesis

The first glasses made to test in the system were lithium meta-phosphate glasses, $LiPO_3$, similar to those synthesized in the literature [24, 25, 27-30, 33]. These glasses were made outside of a glovebox by first weighing out stoichiometric amounts of lithium carbonate and ammonium phosphate dibasic in an alumina crucible and later a platinum crucible. The first method for melting and calcining this raw materials mix was to heat the batch in an alumina crucible to 1000°C for 30 minutes after which it was weighed to check the calcined mass lost. The melt then was put back into the furnace for 5 minutes and cast onto a brass plate. After seeing signs of potential fast melting from calcining too quickly, this casting was switched to melting in a platinum crucible over a Bunsen burner to calcine in a more controlled manner. This melt was then put back in the furnace for 5

minutes and cast on a brass plate. In both methods, the glass is brought into the glovebox due to the slightly hydroscopic nature of the glass.

ii. Glove box synthesis

The majority of sulfide glasses were made in in tube furnaces hermetically sealed to an N_2 atmosphere. Starting material sulfide powders were weighed out in stoichiometric amounts using a balance in 3-10g batches. The batch was then placed in a stainless steel Spex mill pot and ball milled for 30 minutes. The milled powder was then weighed in a glassy carbon crucible and melted for 5-10 minutes between 650-900°C depending on the composition. The crucible and melt were then weighed again on the balance to measure a weight loss of the glass melt. The melt was then put back in the furnace for 3-5 minutes at the same temperature and then poured out and splat quenched between two brass plates forming a glass or ceramic depending on a fast enough quench rate. For conductivity discs the melt at this point was poured into a brass mold heated to 50°C below the glass's T_g and held at that temperature for 45 minutes to anneal the glass then the mold temperature was dropped to room temperature 1 degree per minute.

iii. Planetary milled sulfide glasses

A zirconia mill pot using approximately 20 mill balls was used to synthesize highly volatile or poor glass forming compositions to prevent large mass losses. The starting sulfide glass materials were weighed out in stoichiometric amounts in the glove box and added to the zirconia mill pot. The mill pot was then taken out of the glove box and placed in a Fritsch planetary ball mill and run at 350 rpm for 20 hours, switching

direction every half hour to prevent build up in the mill pot. Once done milling, the mill pot was brought back into the glove box and the glass powder is scrapped out for analysis or further experiments.

C. Nitriding Procedure

The first step for nitriding both oxide and sulfide glasses is to in the glove box weigh out the base glass composition in individual reusable vitreous carbon crucibles and place them on a graphite boat pictured in Figure 5, into a plastic bag. Once sealed, the bag is taken out of the glovebox and brought to the ammonolysis furnace. Beforehand the water cooling line valves were opened and the furnace program was set for the desired temperature, duration, and ramp rates. The graphite furnace boat is then taken out of the bag and placed in the middle of the furnace inside the furnace tube and promptly the furnace is closed. During this time the glasses are exposed to air before the furnace tube is purged. At this point, the furnace program ramp is started and the nitrogen gas flow is immediately started to purge the furnace while the furnace ramps (30 minutes to one hour). At the desired temperature between 600°C and 850°C the nitrogen inlet valve is closed and the ammonia valve is opened at a rate of 500mL/min and is either held at this rate or reduced to 200mL/min 75 minutes into the ammonolysis time between 2 to 12 hours. At the end of this time, the gas flow was then switched back to nitrogen as the furnace cooled to maintain an inert atmosphere. Once cooled to room temperature, the gas flow was turned off and the samples were removed from the furnace and brought back into the glove box where their weight losses were measured.

Figure 5 – Graphite boat and glassy carbon crucibles used for nitriding glasses containing nitrided lithium phosphate glass.

D. Nitrogen Analysis

i. Combustion analysis

The nitrogen elemental analysis results (%N) were acquired using a PE 2100 Series II combustion analyzer (Perkin Elmer Inc., Waltham, MA). The instrument works by combusting samples in a sample chamber and analyzing the gases for carbon, hydrogen, nitrogen, and sulfur by measuring the CO_2, H_2O, N_xO_y, copper reduced to N_2, and SO_2 present respectively along with the excess oxygen being reduced by the same copper reduction tube. The combustion and reduction temperatures for CHN measurements are 925 ^oC and 640 ^oC respectively, and for CHNS measurements 975 ^oC and 975 ^oC, respectively. The gases are then analyzed using a gas chromatography column, which requires calibration due to columns in the system having adsorption and desorption sites that must be in equilibrium. To establish the steady state of the instrument and calibrate for the elements of interest a sequence of blanks, standards, and samples are run in tin sample capsules sealing 2-4 mg of samples weighed using a

microbalance. In CHN mode, acetanilide is used as a standard for calibration and for CHNS cysteine is used. The standards and reagents were from Perkin Elmer and Elementar America's Inc. When run according to the sequence, +/- 0.3% accuracy can be achieved for each element. The first runs on oxide glasses were performed using CHN elemental measurements and later sulfide glass measurements were attempted using CHNS measurements. CHNS analysis was unsuccessful due to the sulfide glasses high sulfur content oversaturating the reduction tubes and distorting the percentages of all elements.

ii. X-Ray photoelectron spectroscopy

XPS analysis was performed as a more accurate technique for sulfide containing glasses due to the high sulfur content being detrimental to the results on the combustion analysis. Samples were sent to the Iowa State Materials Analysis and Research Lab (MARL) for analysis on a Kratos Amicus/ESCA 3400 instrument by being loaded in an airtight sample holder in our glove box. To fit inside the holder, a single smooth flat glass sample of under 10 by 10 mm dimensions and 5 mm thickness was loaded in the sample holder. The sample holder was taken out of the glove box and brought back to the Kratos Amicus/ESCA 3400 instrument. The sample was then loaded into the instrument and pumped down to ultra high vacuum. The sample was irradiated with 240 W unmonochromated Mg $K\alpha$ x-rays, and the photoelectrons emitted at 0° from the surface normal were energy analyzed using a DuPont type analyzer. The pass energy was set at 150 eV and either a Shirley or linear baseline was removed from all reported spectra. CasaXPS software was used to process raw data files.

iii. IR spectroscopy

IR spectroscopy was performed on glass and crystalline samples by first making a powder of the glass sample of interest in a mortar and pestle. Next 3-8 mg of ground glass sample are weighed out and mixed with 0.200 g of cesium iodide and pressed in a metal die into a pellet in the glove box. The sample pellets are then put in a jar and taken out of the glove box and transferred to an antechamber connected to a Bruker IFS 66v/s Fourier transform infrared spectrometer that was flushed with nitrogen. A cesium iodide background is run followed by samples run on OPUS software and used to observe oxygen, water, inorganic, and sulfide contamination. The sample pellets had acquisitions of 4 cm^{-1} resolution and 32 scans from 100 to 4000 cm^{-1} covering primarily the mid infrared range.

iv. Raman spectroscopy

For Raman analysis, either powders are pressed into flat discs or splat quenched glass shards sealed with vacuum grease between a polymer holder and silica glass slide while inside a glove box. The sealed slide then is taken out of the glove box and is taken to the Renishaw micro- Raman Dispersive Spectrometer. The 488 nm Ar- ion laser source is turned on, followed by the stage motors, and WIRE software. The sample was then focused on using either 5x or 20x objective lenses and spectra were acquired in most cases using 100% laser power, 10-20 acquisitions, and 10-20 second scans each acquisition. These scans were then repeated and acquisitions changed and retaken to get representative high signal to noise Raman spectra.

v. Differential scanning calorimetry

For thermal analysis of the glasses a Perkin Elmer DSC Pyris Diamond was used to identify the Tg and Tc temperatures for each composition. Glass samples were sealed as 5- 15 mg of glass powder or glass pieces in an aluminum sample pan inside the glove box. The loaded sample pans were weighed out on a microbalance and pan weights were subtracted to obtain sample weights. The sample pan was loaded in the DSC sample holder and run from room temperature to 450°C as a survey scan. A second sample pan is loaded and cycled around the glass transition point seen in the survey scan to achieve repeated data relieving stresses in the glass. After the sample is run, an empty aluminum sample pan is run in the DSC at the same rate and temperature range to create a baseline subtraction.

vi. Impedance spectroscopy

First, a cast annealed disc (approximately 25 mm diameter) of the desired composition was polished flat and optically clear, starting with 180 grit sandpaper and progressing to higher grits and ending with 4000 grit alumina polishing papers. Once both sides are parallel and flat a 10 - 15 mm diameter gold sputtered or silver paint electrode is applied to both sides of the polished glass disc. Next, the nitrided lithium phosphate glasses with electrodes were placed between 0.5 mm brass blocking electrodes with tweezers in a Novocontrol Technologies Concept 80 Impedance Analyzer. The samples were run from 303 K (30 °C) to 443- 523 K (170-250 °C) from 10 MHz to 0.1 Hz, where the temperature was held at ±0.5K for each set point and held for 3-5 minutes before sampling. The dc impedance lithium ion conductivity of these curves were then

found by fitting the curves and separating out the real component of the complex impedance using Equation 5 [72]. The ω term is the angular frequency, n is an exponent term between 0-1, and Q is a constant phase element in parallel to the lithium ion conducting glass.

$$Z^*(\omega) = Z'(\omega) - iZ''(\omega) = \frac{R}{1 + RQ(i\omega)^n} \tag{5}$$

$$\sigma_{d.c.} = \left(\frac{1}{R}\right)\left(\frac{t}{A}\right) \tag{6}$$

Equation (6) was used to convert the resistance to dc conductivity, $\sigma_{d.c.}$, using the glass thickness (t), electrode area (A), and resistance (R) from equation 5. Activation energies then are determined by fitting the dc ionic conductivities to an Arrhenius plot of the conductivity with temperature and achieving a linear fit.

CHAPTER 4. RESULTS

The first nitriding performed with the ammonolysis system was lithium phosphate, $LiPO_3$, glass on which previous research had been performed on the thermal, mechanical, and conductive properties of the glass. Next sulfide glasses were nitrided in the system in the lithium oxy-thio borate system and a few sodium oxy-sulfide glasses that had mixed glass formers. The results from these nitridation experiments is presented starting with their nitrogen uptake, then both their Raman and IR structural results, followed by thermal analysis, and impedance spectroscopy. Each section the glasses will be presented in the order nitrided oxide and then sulfide glasses.

A. Nitrogen analysis of Glasses

i. Combustion Analysis

Results of the PE 2100 Series II combustion analysis of the lithium metaphosphate glass show the success of the nitridation of the glass in that there is nitrogen in the glasses, however only very modest amounts of nitrogen were incorporated. Table 1 displays the results from a number of runs and their sample numbers showing the inconsistency of any uptake of nitrogen into the glass network. All have some presence of nitrogen and the same trends seen, but consistently less than 1 wt. % is incorporated. This is less than would be expected according to literature, where very quickly (3-7 hours) more than 1 % is incorporated, along with there not being much consistency between the same samples analyzed by Munoz et al. [1]. Once working with sulfides the PE 2100 Series II combustion analyzer was unable to handle the amount of

sulfur present in the glasses in reduction tubes and still be able to obtain accurate measurements of the nitrogen content in the glasses. This led to the need for further analysis to look for a more accurate measurement technique.

Table 1- Nitrogen content results from PE 2100 Series II combustion analyzer for lithium phosphate glasses, along with comparison results from Francisco Munoz lab.

Time Length	Temperature	Flow Rate (NH_3)	ISU Average			Munoz [1]		
		mL/min	%C	%H	%N	%C	%H	%N
2 hour graphite crucible	700°C	~1335	0.02	-0.04	0.38	0.21	0.08	0.94
2 hour	700°C	~1335	-0.01	-0.08	0.29	0.01	0.02	0.16
4 hour	700°C	~500	0.02	-0.04	0.57	0.10	0.04	1.55
6 hour	700°C	~500	-0.04	-0.04	0.49			
~4 hour	750°C	~500 for 75 minutes, then ~200 N_2 flow left on	-0.04	-0.05	0.58			
4 hour	750°C	~500 for 75 minutes, then ~200	-0.03	-0.06	0.54			
6 hour	750°C	~500 for 75 minutes, then ~200	-0.01	-0.04	3.30			
			0.00	0.04	0.44			
12 hour	750°C	~500 for 75 minutes, then ~200	0.05	0.01	0.77			
			0.01	0.03	0.87			
			0.04	0.00	0.59			
			0.01	0.04	0.63			
			0.04	0.01	0.53			

ii. X-Ray Photoelectron Spectroscopy

To better determine compositions and the uptake of nitrogen in sulfide glasses, XPS analysis was incorporated in the analysis of the glasses. To first compare and prove the viability of the method for composition analysis lithium metaphosphate glasses were analyzed which had previously been analyzed by combustion analysis. A sample of LiPON that was nitrided for 12 hours in the ammonolysis furnace was loaded and analyzed both as fractured and polished similar to conductivity samples in case signal differed depending on how rough the sample surface was. Figure 6 has an example XPS elemental binding energy spectrum displayed from a 12 hour nitride ammonolysis run both sputter cleaned and uncleaned showing how the cleaning diminishes the contaminate carbon. Figure 7 displays narrow scans of the binding energy range for nitrogen 1s for the 12 hour LiPON samples run. There is variability between samples but it is apparent that there are two different environments present in the glass, present from different bonding environments of the nitrogen whether double or triple coordinated. In work by Bates et. al., nitrogen 1s peaks were identified as double coordinated P-N=P at 398.4 eV, triply coordinated  at 399.8 eV, and proposed a possible additional O-N=O peak at 403.4 eV [48]. The 12 hour LiPON sample shows slightly different peak locations with what would be presumed to be the triple coordinated peak being closer 401 eV. A possible reason for this is the work by the Bates group used sputtered LiPON samples rather than ammonolysis. An additional possibility from work by the Day group with ultra-phosphate glass saw a peak near 402 eV attributed to NH_2 groups [29].

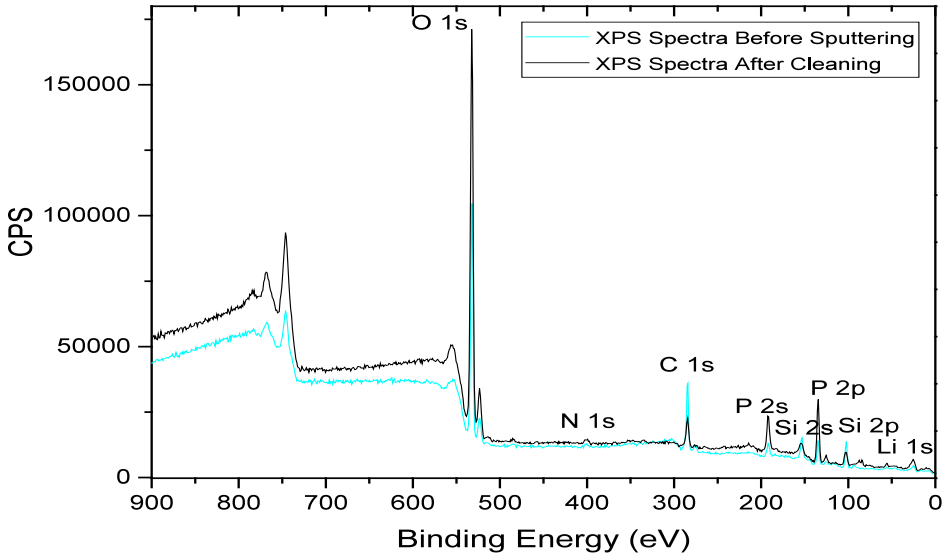

Figure 6- XPS binding energy spectrum of 12 hour nitrided lithium metaphosphate with sputter cleaning and without.

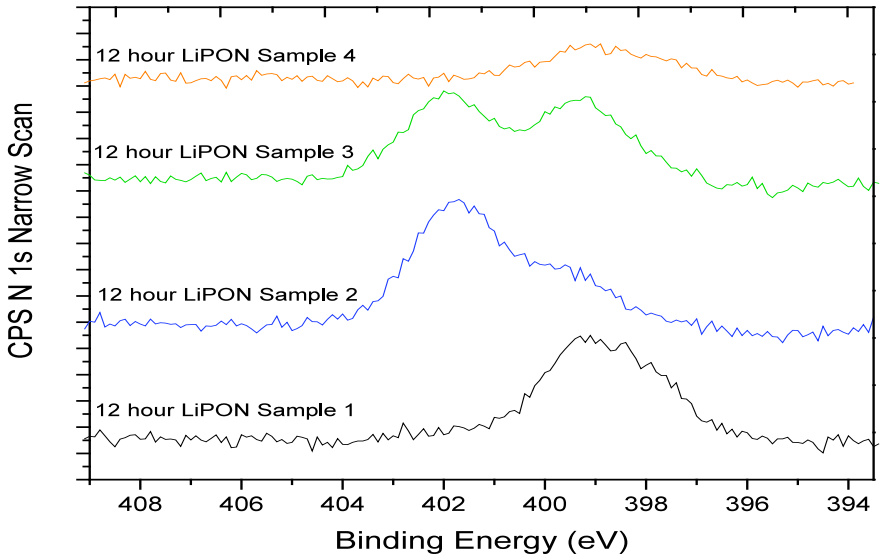

Figure 7- XPS binding energy spectrum of 12 hour nitrided lithium metaphosphate with sputter cleaning (for samples 1, 3, and 4) zoomed in around the binding energy of N 1s electrons.

Table 2 contains the compositional results of the glasses analyzed both oxides and sulfides post nitride. A number of observations are apparent in this table, first even with

sputter cleaning there is carbon surface contaminants present. Second, the oxide nitrogen weight percentages are in the same scale as those by combustion analysis and tend to agree. Third the sulfide results tend show signs of higher than expected oxide content in sulfide starting materials and presence in the carbon molecular contamination, seen in the higher than expected atomic and weight percent of oxygen present. Figure 8 contains the XPS spectra of lithium thio-borate glass nitrided for 4 hours and then requenched to a glass inside the glove box. The sputter cleaning of the glass surface clearly brings out the peaks of the sulfur and boron characteristic binding energies. Also there are two oxygen environments due to there being two distinct peaks in the spectra.

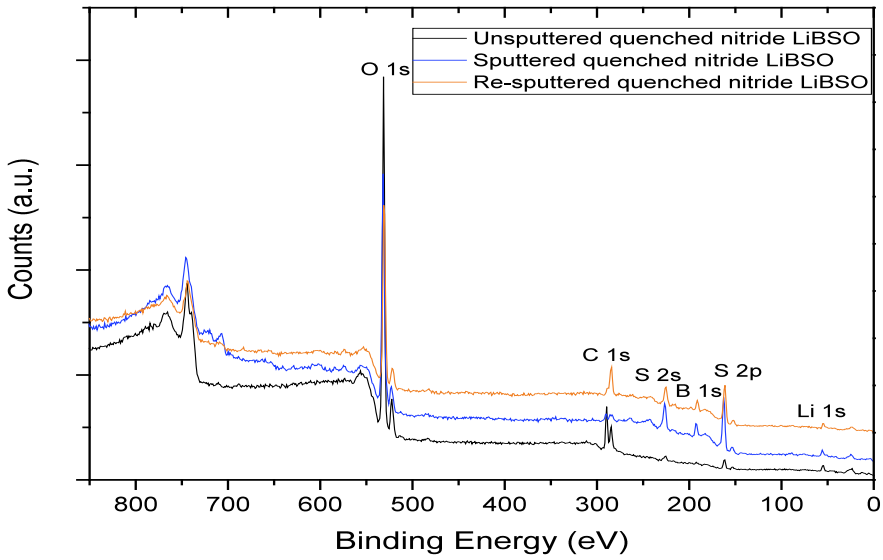

Figure 8- XPS binding energy spectrum of remelted 4 hour nitrided 0.70 Li_2S-0.27B_2S_3-0.03B_2O_3 glass showing no peak for N 1s binding energy.

Table 2- Composition of LiPON and nitrided lithium thio-borate glass samples as measured by XPS analysis.

Sample		Sample 1			Sample 2			Sample 3			Sample 3		
		Position (eV)	% At. Con	% wt.	Position (eV)	% At. Conc.	% wt.	Position (eV)	% At. Conc.	% wt.	Position (eV)	% At. Conc.	% wt.
12 hour nitride $LiPO_3$	O 1s	531.5	59.15	56.41	531.4	58.98	56.00	531.7	61.25	60.00	531.1	58.89	57.13
	N 1s	399.1	0.81	0.68	401.7	0.93	0.77	402.0	1.08	0.92	398.9	0.25	0.22
	C 1s	284.6	11.50	8.23	284.6	7.76	5.53	284.6	14.19	10.44	284.6	11.13	8.10
	P 2p	134.3	14.49	26.75	134.4	17.10	31.43	134.3	12.68	24.05	134.4	13.89	26.09
	Li 1s	55.4	12.98	5.37	55.4	15.23	6.27	55.5	10.79	4.59	55.7	14.94	6.29
	Ca 2p	347.5	1.07	2.56							347.3	0.89	2.17
4 hour nitride $0.70Li_2S$-$0.27B_2S_3$-$0.03B_2O_3$ remelted		unsputtered			sputtered			2nd sputter					
		Position (eV)	At. Conc. %	wt. %	Position (eV)	At. Conc. %	wt. %	Position (eV)	At. Conc. %	wt. %			
	O 1s	531.2	50.02	61.76	530.8	38.35	43.17	531.8	40.23	41.45			
	C 1s	289.5	20.49	18.99	284.5	19.12	16.15	284.6	7.16	5.54			
	B 1s	191.4	0.90	0.75	191.4	8.00	6.67	191.7	12.78	10.66			
	S 2p	161.4	1.65	4.07	161.2	10.04	22.63	161.4	16.27	33.59			
	Li 1s	55.1	26.95	14.43	54.9	24.49	11.96	54.7	23.57	10.53			

B. Structural Analysis of Nitrided Glasses

i. IR Spectroscopy

Infrared spectroscopy was performed on powders of both the glass and crystallized samples, allowing comparison to both literature and the success of nitridation of the glasses. Broadly, Figure 9 makes visible the variability in IR spectra of the nitrided lithium metaphosphate glasses, where both the 2 and 4 hour samples visibly show additional peaks to those seen in the base $LiPO_3$ glass and 6 hour nitrided samples.

The broad peaks contain several characteristic vibrations to lithium metaphosphate including non-bridging P=O bonds at approximately 1270 and when the electronegativity of the groups bonded to P decrease (nitrogen substitution), the vibration shifts to lower wavenumbers and a strong peak at 1176 cm^{-1} with nitrided samples [27, 77]. In the nitrided spectra in Figure 9 there is a slight shift of these two peaks to lower wavenumbers, particularly the 1176 cm^{-1} shift where the peak seems to slide into the bulk other vibrations. At 1100 cm^{-1} a $P\text{-}O^-$ stretching mode is assigned which can be seen being obscured as the P=O mode shifts into it due to nitrogen incorporation [77]. Several peaks are identified tentatively as being related to P-O-P vibrations, first at 898 cm^{-1} that shifts to higher wavenumbers upon nitrogen incorporation, and two P-O-P peaks at 740 and 790 cm^{-1} that broaden upon nitrogen being present [27]. The 2 and 6 hour both show possible signs of broadening and a shift in the 898 cm^{-1} peak, but the 4 hour nitrided sample seems to show more distinct peaks either of contamination or crystallinity.

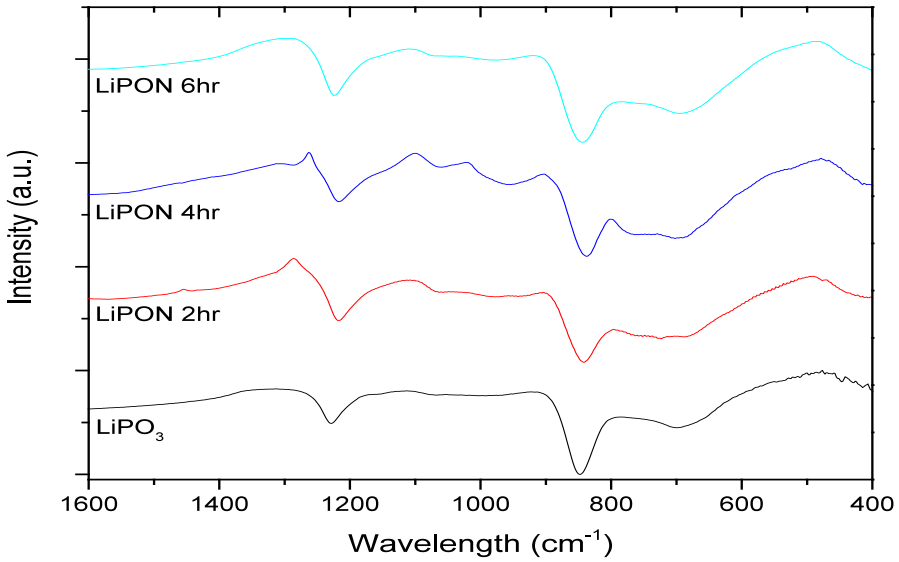

Figure 9- Infrared spectroscopy comparison of base lithium metaphosphate, 6 hour nitrided lithium metaphosphate, and 12 hour nitrided lithium metaphosphate samples run in vitreous carbon crucibles.

When nitriding the $0.70Li_2S$-$0.27B_2S_3$-$0.03B_2O_3$ glass, the small working range of the glass became a hindrance to forming nitrided glasses by ammonolysis. A solution sought for this problem was to in a nitrogen atmosphere glove box, remelt and quench the crystallized ammonolysis product. Figure 10 shows both the base glass in a polished state that is a dark red color and the crystallized ammonolysis product from letting the furnace free fall after the end of the synthesis run resulting in a crystalline product. The crystallized product clearly shows two regions a top third that is darker and more bubble filled and the bottom two-thirds that is a more light brown in color. Likely meaning the ammonia is reacting with the top of the melt in the crucible.

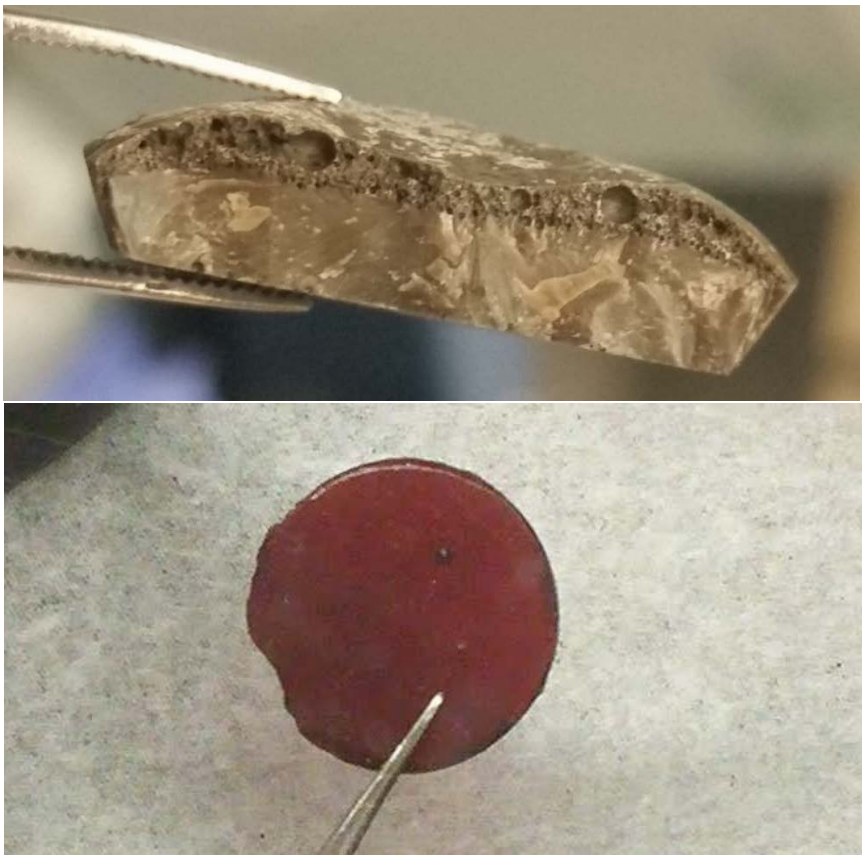

Figure 10- Above- Crystallized 6 hour nitrided 0.70 Li_2S - 0.27 B_2S_3 - 0.03 B_2O_3 disc showing surface bubbling and crystallization. Below- Polished base 0.70 Li_2S - 0.27 B_2S_3 - 0.03 B_2O_3 glass.

Figure 11 contains four IR spectra illustrating the results and issues with nitriding this glass. It is clear that there is minimal difference between the base oxy-sulfide glass and the melted version, so if there was any nitrogen incorporation in the glass network it either is very minimal or has left the glass upon remelting. The two post-ammonolysis spectra from the crystallized nitridation product show very little glassy character, having distinct peaks rather than broad glassy vibrations in the same locations seen in the glassy samples.

The base lithium thio-borate glass and nitrided products have a number of characteristic stretches that can be identified and aid in understanding if there has been

any change upon nitridation in the glass. The peaks between 800-900 cm^{-1} correspond to trigonal boron sulfide groups, where the distinct peak closer to 900 cm^{-1} are part of thio-boroxyl ring structures and the peak closer to 800 cm^{-1} are loose trigonal BS_3^{-3} [78]. Above 1000 cm^{-1} are boron oxide related vibrations asymmetric stretching of BO_3^{-3} at around 1300 cm^{-1}, pyroborate units at 1130 cm^{-1}, and BO^{4-} tetrahedral at 1040 and 960 cm^{-1} [79, 80]. There potentially could be a boron nitride related vibration in this region too but the small size of either peak would make it difficult to identify. The characteristic peaks for hexagonal boron nitride are a strong vibration at 1367 cm^{-1} corresponding to B-N asymmetric stretching, and a weaker B-N-B bending vibration at 783 cm^{-1} [81].

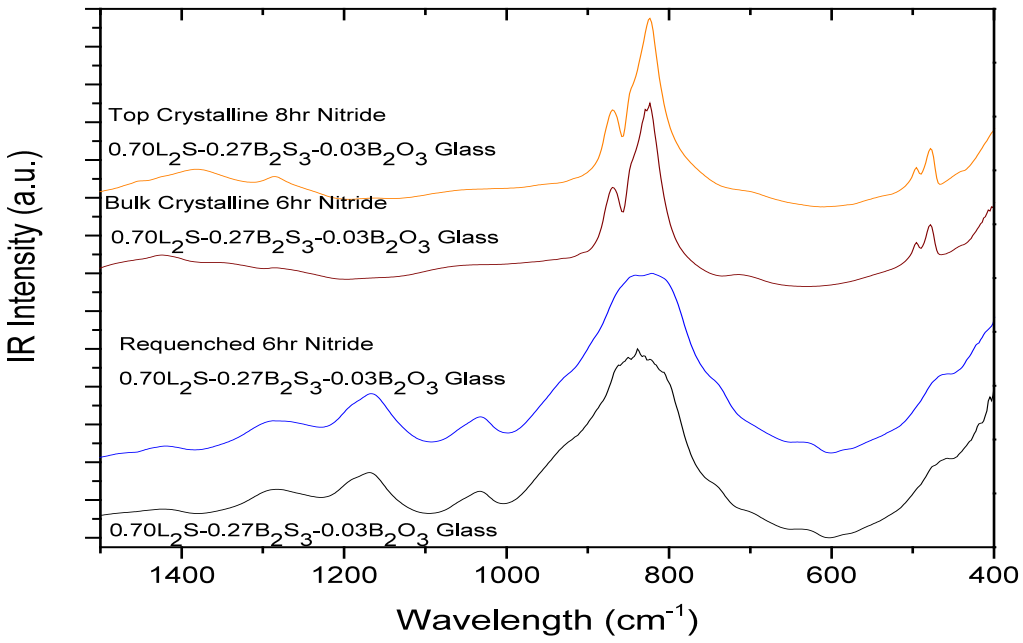

Figure 11- Infrared spectroscopy comparison of 0.70 Li_2S- 0.27 B_2S_3- 0.03 B_2O_3 glass, 6 hour nitrided of 0.70 Li_2S- 0.27 B_2S_3- 0.03 B_2O_3 crystallized, 8 hour nitrided of 0.70 Li_2S- 0.27 B_2S_3- 0.03 B_2O_3 crystallized and remelted 6 hour nitrided of 0.70 Li_2S- 0.27 B_2S_3- 0.03 B_2O_3 glass.

ii. Raman spectroscopy

Additional structural analysis of the glasses was performed using Raman spectroscopy. Figure 13 displays a comparison of the LiPON glasses and those that were not nitrided to investigate the changes to P-O-P bonding with the incorporation of nitrogen to the glass network. Due to the low uptake of nitrogen, the presence of nitrogen in the glass network is hard to discern. Table 4 outlines the vibrations of important bonds in the structure of lithium metaphosphate glass, of importance are the P-O-P related peaks where the peak around 700 cm^{-1} where nitrogen atoms substitute oxygen atoms [36]. In Figure 12 there looks to be evidence in the top 6 hour nitrided sample of triple coordinated nitrogen around 600 cm^{-1}, but less apparent double coordinated nitrogen at 830 cm^{-1}as identified in Table 3 [36]. Additionally both O-P-O and P=O stretches can be seen in all three spectra as identified by Table 4.

Table 3- Raman shifts of characteristic peaks in Raman spectra of base lithium metaphosphate glasses and those that were nitrided.

Peak Assignment	Raman Shift (cm-1)
P=O	1250
P-O-P	735
P=N-P	830
P-N<$(P)_2$	630
P2O74-	1020
O-P-O	1170

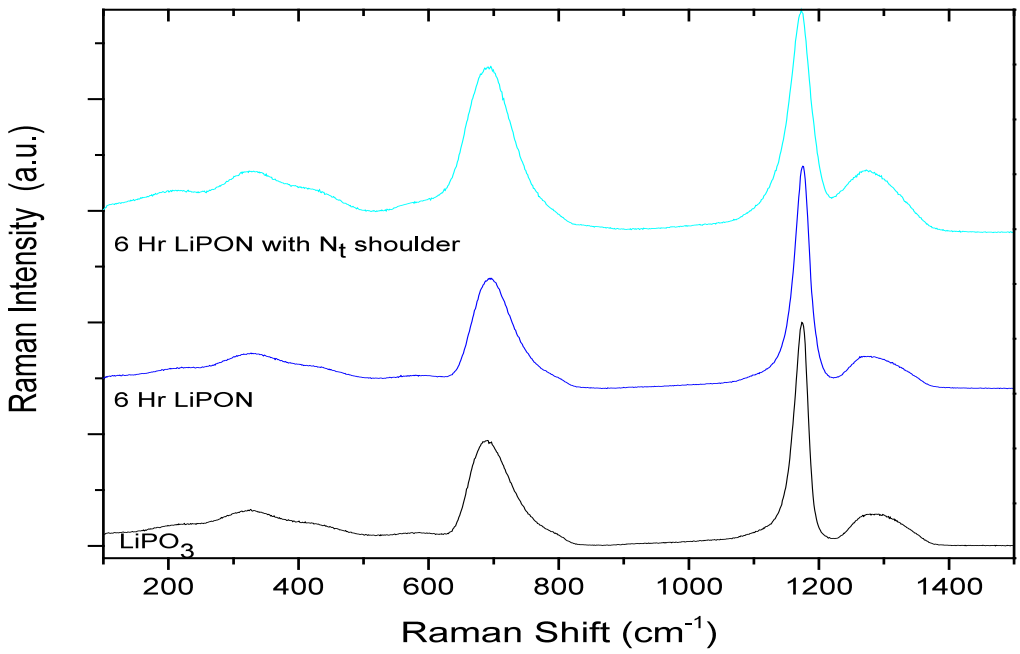

Figure 12- Raman spectra comparison of base lithium phosphate, $LiPO_3$, glass and 6 hour nitrided lithium phosphate glass.

Similar to the IR spectroscopy, the Raman spectra of the $0.70Li_2S$-$0.27B_2S_3$-$0.03B_2O_3$ glass and nitrided products Figure 13 displays the minimal difference between the base glass and remelted nitrided product. Additionally it is clear by the distinct individual peaks that the crystalline product has a similar composition, but is made up of individual crystalline Raman shifts rather than the individual shifts being combined into broad ranges as in the glassy starting material. The peaks primarily in the 400-500 cm^{-1} Raman shift region show the composition to be made up of 6 membered rings of mostly boron sulfide along with some boron oxide present as to be expected.

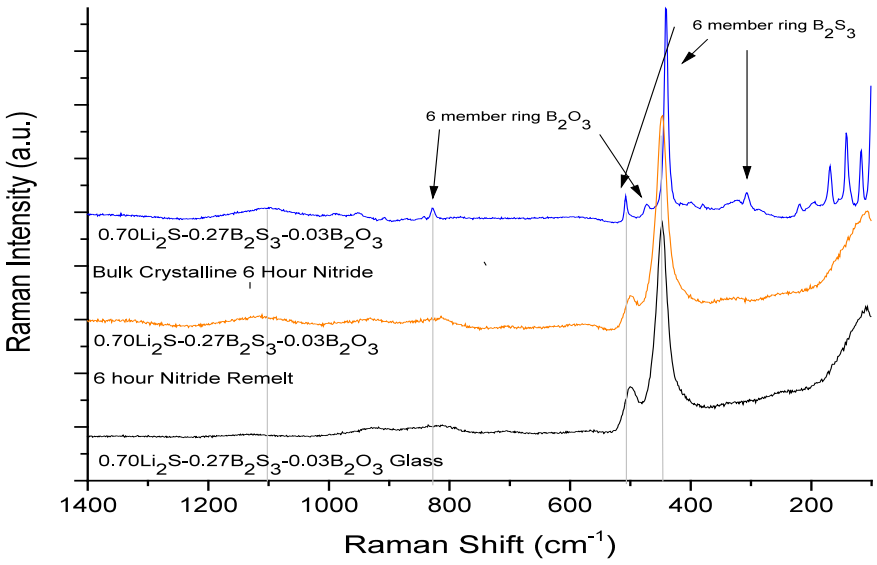

Figure 13- Raman spectra comparison of 0.70 Li_2S- 0.27 B_2S_3- 0.03 B_2O_3 glass compared with nitrided products of the glass.

The Raman spectra of crystallized products from the nitriding of the lithium oxy-thio borate glass are compared in Figure 14. Several interesting things become clear, first that the bulk crystallized product resembles the glassy samples of the same composition, but the top layer of the 8 hour crystallized nitrided samples, show significant phase separation due to their varied spectra. The top layers of the nitrided product samples show a large number of Raman peaks and what looks to be a higher oxide content. One additionally issue with these surface layers as seen in Figure 10 is the darker, bubble filled surface layer would most likely contain nitrogen from the ammonolysis of the glass. Figure 14 contains a spectrum of boron nitride for comparison of potential bonding of nitrogen to the boron glass former. This leaves a complex Raman spectra that shows no hexagonal boron nitride peak, but leaves a large number of oxide and sulfide peaks.

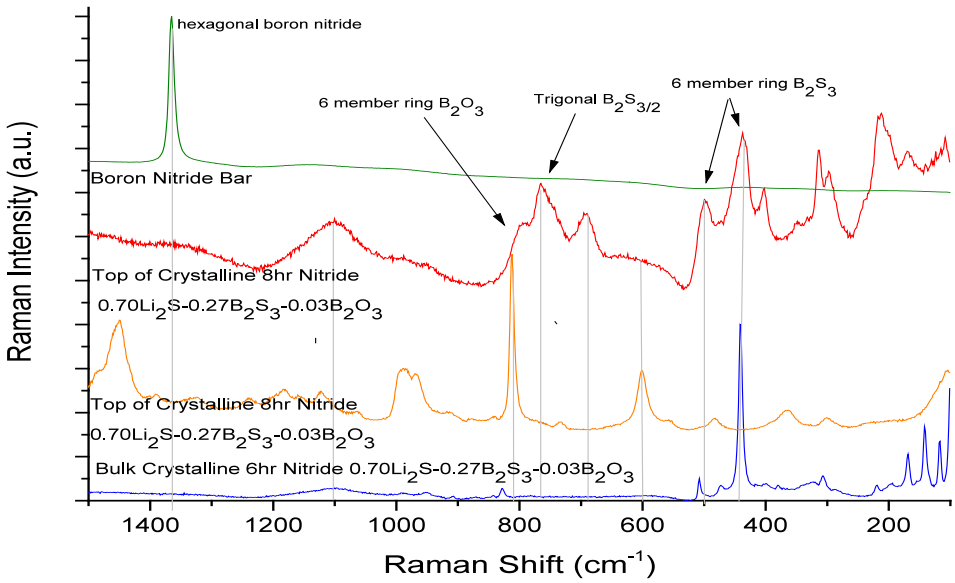

Figure 14- Raman spectra comparison of 0.70 Li_2S- 0.27 B_2S_3- 0.03 B_2O_3 glass compared to the crystalline nitrided products.

iii. Differential Scanning Calorimetry

The ammonolysis of the lithium phosphate glasses showed a significant change in Tg from that of the base glass. Table 4 displays the length, temperature, and flow rate of ammonolysis runs along with the Tgs of the glasses. The table shows variability between runs in the success of the nitridation seen in how there can be 10-20 °C differences in Tg temperature for the same ammonolysis time. Figure 15 compares the DSC curves of the base lithium phosphate glass to that of a glass nitrided for 2 hours. A short time span nitriding the glass results in a 40-50 degree Tg increase simply through nitrogen incorporation in the glass network. The ammonolysis runs done show minimal signs of coherent trends. This is noticeable by how longer runs using the same temperature and ammonia flow rate may have lower Tgs relative to the shorter counterparts. One possible

interesting nitrided sample is the 4 hour run where the ammonia flow was accidently switched to a slow flow of nitrogen rather than simply slowing the ammonia flow.

Table 4- Parameters and Tgs of lithium phosphate ammonolysis runs.

Time Length	Temperature	Flow Rate (NH3)	Tg (°C)	
		mL/min	Sample 1	Sample 2
2 hour	700 °C	~1335	353	
			351.3	
			349.5	
2 hour	700 °C	~1335	361.3	357.4
			358.1	354.5
			357.7	355.3
4 hour	700°C	~500	360.9	357.9
			360.0	357.0
			361.3	356.3
6 hour	700C	~500	331.2	
			315.8	
			326.7	
~4 hour	750°C	~500 for 75 minutes, then ~200 N2 flow left on	385.2	
			381.1	
			382.1	
4 hour	750°C	~500 for 75 minutes, then ~200	333.3	
			334.4	
			334.6	
6 hour	750C	~500 for 75 minutes, then ~200	349.8	
			346.0	
			345.6	

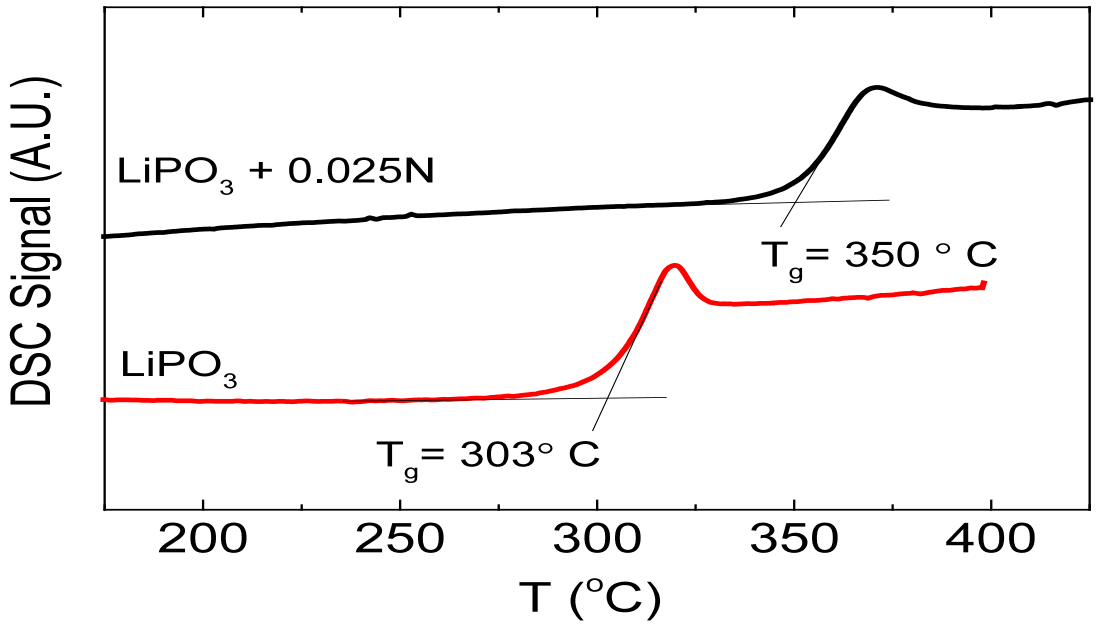

Figure 15- DSC comparison of base lithium phosphate glass and 2 hour nitrided lithium phosphate glass.

iv. Impedance Analysis Results

The impedance analysis results show unexpected results relative to existing literature trends showing gains in LiPON lithium ion conductivity. The lab synthesized LiPON samples of various length ammonolysis runs despite positive Tg increases have either losses in conductivity or minimal changes. Figure 16 shows that all nitrided glasses have a lower conductivity relative to the base LiPON glass with the 4hr nitrided glass that was switched to back to nitrogen after 75 minutes of the synthesis run being about the same as $LiPO_3$. Some possible reasons for these glasses not having a boost in conductivity are bad base $LiPO_3$ synthesis and the significant presence of bubbles in synthesized glasses. Table 5 displays conductivities and activation energies for all glasses run displaying how most are worse than the base glass.

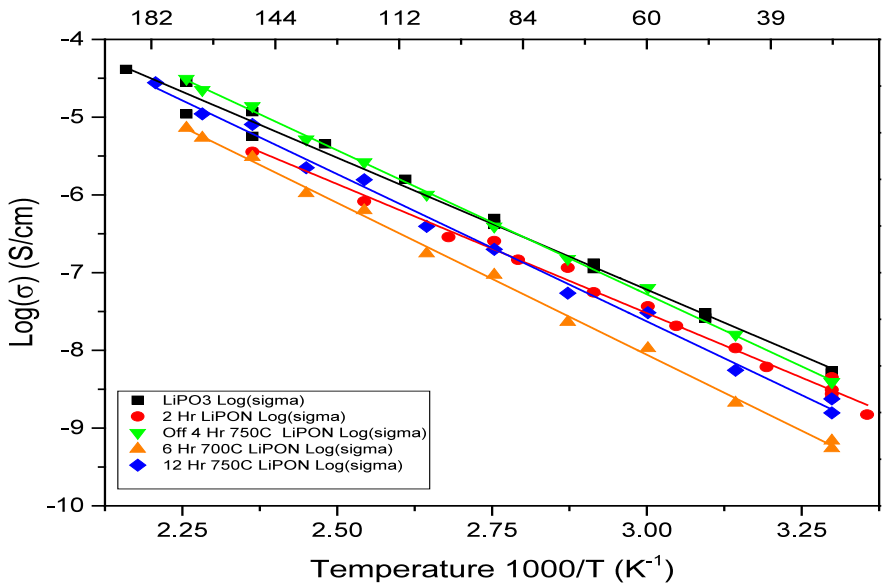

Figure 17- Arrhenius fits of LiPON lithium ion conductivity as a function temperature for various lengths of ammonolysis runs.

Table 5- LiPON glass conductivities and activation energies

Time	Temperature	Flow Rate (NH3)	$Log_{10}(\sigma)$(S/cm)		Activation Energy	
		mL/min	T(150°C)	T(30°C)	(eV)	(kJ/mol)
0 hour	N/A	N/A	-4.93	-8.26	0.71	68.51
2 hour	700°C	~1335	-5.44	-8.56	0.68	65.6
4 hour	750°C	~500 for 75 minutes, then ~200	-5.39	-8.98	0.79	76.57
~4 hour	750°C	~500 for 75 minutes, then ~200 N2 flow left on	-4.86	-8.41	0.77	73.98
6 hour	700°C	~500	-4.93	-8.26	0.69	66.91
6 hour	750°C	~500 for 75 minutes, then ~200	-5.34	-8.76	0.76	72.86
12 hour	750°C	~500 for 75 minutes, then ~200	-5.09	-8.62	0.78	75.59

CHAPTER 5. DISCUSSION

A. Comparison to previous lithium phosphate literature

The nitrided lithium phosphate glasses showed almost no structural changes to the base glass and displayed minimal signs of IR and Raman structural unit changes due to nitrogen incorporation in the glass network. This is to be expected when compared with literature, where most definitive signs of structural changes occur past 5 weight percent incorporation and none of the nitrided glasses upon analysis either from combustion or XPS showed more than 2 weight percent nitrogen. The most promising and similar to previous literature results were the thermal property changes seen by an increase in their T_{gs}. Their conductivities though greatly differed from the small increase in ionic conductivity seen in literature upon nitridation, and instead have what appears to be a negligible or negative effect.

i. Minimal nitrogen uptake

The minimal or few weight percent uptake of nitrogen in the glass network was unexpected relative to similar ammonolysis experiments in previous literature. Experimental procedures for these papers detail information such as their flow rates, gas used, ammonolysis temperature, ammonolysis duration, and appearance however still leave out helpful details for replication. Key omissions are how big their synthesis chamber is rendering flow rate only partial helpful, furnace ramp rates along with intricacies of getting to and from ammonolysis processing to air and room temperature. These makes it difficult infer what is causing the nitrided glasses to have trapped bubbles in bulk synthesis, opposite of descriptions stated in literature. The bubbles are then a

potential cause of the poor increase in nitrogen content and in turn ionic conductivity for the length of time of ammonolysis, due to them being the most prominent difference by description between the literature and the glasses presented here.

ii. Best nitridation outcome

The best results when nitriding the lithium metaphosphate glasses is when instead of switching the ammonia flow to a slower flow rate at 75 minutes in, the ammonia flow was switched to nitrogen for the remainder of the 4 hour synthesis time at the full furnace temperature. The nitrided glass here performed better than its counterpart that was under ammonia flow for the whole 4 hour ammonolysis time. The flow of nitrogen at the ammonolysis temperature likely allowed the release of trapped bubbles in the glass melts that had formed during ammonolysis. Removing the bubbles may lead to a more dense glass leading to better ionic conductivity. Further investigation will be needed to determine the best gas and temperature profile for optimal nitrogen incorporation in the nitrided glasses, but allowing nitrogen to purge the system at the ammonolysis temperature in the sample runs is of particular interest.

iii. Glass transition temperature

The significant immediate increase in glass transition temperature of the nitrided lithium metaphosophate glasses seems to indicate that even a little tightening of the glass network greatly changes the thermal properties of the glass. Since these glasses show 0-4 wt. % nitrogen and barely perceptible IR and Raman signatures, the increases in glass

transition temperature are the most noticeable evidence of nitrogen incorporation. This may occur due to thermal properties being dependent only on the presence of some nitrided sites in the glass network, while ionic conductivity is reliant on a percolation threshold where there is enough nitrided sites to create a path through the glass for conduction.

iv. Ionic conductivity

The negligible change or lower lithium ion conductivity in the nitrided lithium metaphosphate glasses is an unexpected outcome relative to what was expected from previous research groups. Two probable reasons for this could be the low nitrogen content and the large number of bubbles along the crucible surface. Crucibles showed no evidence of degradation into the glass melt from attack by either the melt or the ammonia atmosphere. The bubbles though may affect the conductivity measurements by creating air voids in the glass being tested, resulting in lower conductivity due to blocking the conducting ions and creating another barrier for conduction. Another possible reason is that at only having less than 2 weight percent nitrogen a critical threshold for better conductivity was not achieved. It would seem that without a critical amount of nitrogen networking in the glass, the gains on the lithium conductivity become unapparent, despite the point for thermal property changes being detectable.

B. Primary Issues Nitriding Lithium Oxy-Thio Borate Glasses

The nitriding of the lithium oxy-thio borate materials made it clear that there are additional challenges to ammonolysis of sulfide glasses stemming from the smaller working range and the different glass formers of the composition nitrided. Along with the poor stability of the glasses, these problems require solving issues regarding nitrogen incorporation, bubble formation, phase separation and crystallization, and base glass thermal stability. Further characterization will be needed to identify what is crystallizing and why nitrogen seems not to be incorporating into the glass network.

i. Poor nitrogen uptake

Like the lithium metaphosphate glasses the lithium oxy-thio borate glasses had minimal nitrogen uptake observed. These glasses though, upon requenching in the glove box showed no XPS N 1s peak leading to there either being no incorporation of nitrogen or that it leaves the melt when the crystalline ammonolysis product is recast. The ammonia is interacting with the product as evidenced by the dark bubble filled layer on top of the crystallized glass ammonolysis product. A possible issue as of yet not fully explored is whether this poor nitrogen uptake is due to the low working range of the lithium oxy-thio borates, having to do with boron being a glass former instead of phosphorus, or a combination of the stronger binding of boron and higher melting temperature of glasses. There could be some variety of instability or chemical viability to the melt imparted by the glass former being boron creating less successful melt conditions compared to other glass formers like silicon and phosphorus.

ii. Crystallization and phase separation

An approximately 30 °C working range of the lithium oxy-thio borate glasses led to poor nitridation due the too the furnace not cooling fast enough to again reach the glassy state upon free fall cooling in the ammonolysis furnace. The result is a dark red crystalline material with a darker bubble ridden layer at the surface that is phase segregated as shown in IR and Raman spectra by comparing the surface layer to the bulk materials. This has led to the need for better glass formers with better working ranges for a more stable melt, more conducive for glass formation for nitridation so as to isolate whether the boron or the poor glass formability is the reason for the poor nitrogen content. An issue with this segregation is the whole glass melt may not be reacting with the ammonia revealed in the dark layers with bubbles as a top layer on crystallized products.

CHAPTER 6. SUMMARY AND CONCLUSIONS

A. Summary

A system was assembled for the ammonolysis of glass samples, with safety and procedural input from EH&S, and aid of FP&M in connecting the system to the building exhaust. First lithium metaphosphate glass samples were nitrided in the system to compare previous studies in literature and the resulting glasses had mixed results. The results were increased Tgs as expected, the glass structure was as expected for a metaphosphate glass, however under 4 weight percent nitrogen was gained in all samples and the samples had bubbles unlike literature. Next ammonolysis of a lithium oxy-thio borate glass was attempted making clear several obstacles to successful nitridation of these sulfide glasses. Issues were seen with measuring nitrogen incorporation in the glass network and with crystallization, segregation, and bubbles in the sulfide glass melt after nitridation. Together, these ammonolysis runs aided in learning what changes to make in the nitridation parameters and future work for successful oxy-sulfide glass nitridation.

B. Conclusions and Future Work

A number of conclusions can be gained from the work with this ammonolysis system, regarding the nitridation of glasses for solid electrolyte applications. The first from nitriding lithium metaphosphate glasses similar to LiPON literature is there are optimal parameters for successful nitridation relating to temperature, ammonia flow, and nitrogen purging. A combination was found that minimized bubble formation in nitrided glasses, high ionic conductivity, and good thermal properties. The best results seemed to be had when the lithium metaphosphate glass was ramped at 1 degree per minute then

held at 750°C with a flow of 500 mL/min for 75 minutes then purging with nitrogen the for a period of hours at 750 °C. Purging with nitrogen for a long period of time at ammonolysis temperature may reduce bubble formation, but needs to be confirmed through more experiments.

One additional conclusion key to this work and future findings is it was found that using combustion analysis became inaccurate with the high sulfur content of the sulfide glasses. This resulted in the need of a different characterization technique; XPS for nitrogen content analysis despite its surface sensitivity, but with etch cleaning the nitrogen content results of the oxide glasses were similar. The drawback to this technique is the low sample throughput and analysis time. Other techniques are difficult to find that are both able to detect nitrogen and work with the mix of elements of interest.

The largest issue seen in both the oxides and oxy-sulfides is poor nitrogen uptake, or in the case of the oxy-sulfides no observed uptake at all. Nitrogen purging the system may help this uptake problem with the oxides, but the lack of definitive evidence of nitrogen in the oxy-sulfides would indicate a larger different issue with nitrogen uptake. Possibilities for this lack of noticeable nitrogen uptake are crystallinity, phase segregation, and incompatibility with the glass network glassformers for nitrogen interaction through ammonolysis. One method in the future to find out if these possibilities are related causes to the nitrogen uptake problem would be to carefully perform phase identification by XRD of the phases present in the crystalline nitridation product., allowing another way to identify the presence of nitrogen in addition to combustion and XPS, determine how the glass melt is crystallizing, and if one phase or another had a preference for the nitrogen. The poor thermal working range of the lithium

oxy-thio borate glass demonstrated by the crystallization issues showed that to nitride a sulfide glass and get a glass to result base glasses with wider working ranges would have to be explored. Some work in the lab has been preliminarily done regarding new compositions showing promise, but potential further issues regarding volatization of the glass melt and still crystallization of the high working range base glasses look to be present and will require further analysis.

REFERENCES

1. Munoz, F., *Nitrogen Containing Samples and Analysis*. 2016.

2. Whittingham, M.S., *History, Evolution, and Future Status of Energy Storage.* Proceedings of the IEEE, 2012. **100**(Special Centennial Issue): p. 1518-1534.

3. Scrosati, B. and J. Garche, *Lithium batteries: Status, prospects and future.* Journal of Power Sources, 2010. **195**(9): p. 2419-2430.

4. Tarascon, J.M. and M. Armand, *Issues and challenges facing rechargeable lithium batteries.* Nature, 2001. **414**(6861): p. 359.

5. Li, J., et al., *Solid Electrolyte: the Key for High-Voltage Lithium Batteries.* Advanced Energy Materials, 2015. **5**(4): p. 1401408-n/a.

6. Nagao, M., et al., *In situ SEM study of a lithium deposition and dissolution mechanism in a bulk-type solid-state cell with a Li2S-P2S5 solid electrolyte.* Physical Chemistry Chemical Physics, 2013. **15**(42): p. 18600-18606.

7. Ren, Y., et al., *Direct observation of lithium dendrites inside garnet-type lithium-ion solid electrolyte.* Electrochemistry Communications, 2015. **57**: p. 27-30.

8. Charles, R.J., *Some Structural and Electrical Properties of Lithium Silicate Glasses.* Journal of the American Ceramic Society, 1963. **46**(5): p. 235-238.

9. Malugani, J.P., et al., *Conductivite ionique dans les verres AgPO3-AgX (X = I.Br.Cl).* Materials Research Bulletin, 1978. **13**(5): p. 427-433.

10. Mercier, R., et al., *Superionic conduction in Li2S - P2S5 - LiI - glasses.* Solid State Ionics, 1981. **5**: p. 663-666.

11. Deshpande, V.K., A. Pradel, and M. Ribes, *The mixed glass former effect in the Li2S : SiS2 : GeS2 system.* Materials Research Bulletin, 1988. **23**(3): p. 379-384.

12. Christensen, R., G. Olson, and S.W. Martin, *Ionic conductivity of mixed glass former 0.35Na(2)O + 0.65[xB(2)O(3) + (1 - x)P(2)O(5)] glasses.* J Phys Chem B, 2013. **117**(51): p. 16577-86.

13. Martin, S.W., C. Bischoff, and K. Schuller, *Composition Dependence of the Na(+) Ion Conductivity in 0.5Na2S + 0.5[xGeS2 + (1 - x)PS5/2] Mixed Glass Former Glasses: A Structural Interpretation of a Negative Mixed Glass Former Effect.* J Phys Chem B, 2015. **119**(51): p. 15738-51.

14. Bischoff, C., et al., *Structural investigations of yNa2S+(1−y)PS5/2 glasses using Raman and infrared spectroscopies.* Journal of Non-Crystalline Solids, 2012. **358**(23): p. 3216-3222.

15. Seino, Y., et al., *A sulphide lithium super ion conductor is superior to liquid ion conductors for use in rechargeable batteries.* Energy Environ. Sci., 2014. **7**(2): p. 627-631.

16. Minami, K., et al., *Electrical and electrochemical properties of glass–ceramic electrolytes in the systems Li2S–P2S5–P2S3 and Li2S–P2S5–P2O5.* Solid State Ionics, 2011. **192**(1): p. 122-125.

17. Minami, K., et al., *Lithium ion conductivity of the Li2S–P2S5 glass-based electrolytes prepared by the melt quenching method.* Solid State Ionics, 2007. **178**(11–12): p. 837-841.

18. Hayashi, A., et al., *Characterization of Li2S–SiS2–Li3MO3 (M=B, Al, Ga and In) oxysulfide glasses and their application to solid state lithium secondary batteries.* Solid State Ionics, 2002. **152**: p. 285-290.

19. Ribes, M., B. Barrau, and J.L. Souquet, *Sulfide glasses: Glass forming region, structure and ionic conduction of glasses in Na2S□XS2 (X□Si; Ge), Na2S□P2S5 and Li2S□GeS2 systems.* Journal of Non-Crystalline Solids, 1980. **38**: p. 271-276.

20. Martin, S.W., *Glass and Glass-Ceramic Sulfide and Oxy-Sulfide Solid Electrolytes*, in *Handbook of Solid State Batteries*

N.J. Dudney, W.C. West, and J. Nanda, Editors. 2015, World Scientific: Singapore. p. 433-502.

21. Muramatsu, H., et al., *Structural change of Li2S–P2S5 sulfide solid electrolytes in the atmosphere.* Solid State Ionics, 2011. **182**(1): p. 116-119.

22. Kim, Y., J. Saienga, and S.W. Martin, *Anomalous Ionic Conductivity Increase in Li2S + GeS2 + GeO2 Glasses.* The Journal of Physical Chemistry B, 2006. **110**(33): p. 16318-16325.

23. Tatsumisago, M., et al., *Structure and properties of lithium ion conducting oxysulfide glasses prepared by rapid quenching.* Solid State Ionics, 1996. **86**: p. 487-490.

24. Brow, R.K., et al., *Surface nitridation of a phosphate glass.* Journal of Non-Crystalline Solids, 1990. **120**(1–3): p. 172-177.

25. Day, D.E., *Structural role of nitrogen in phosphate glasses.* Journal of Non-Crystalline Solids, 1989. **112**(1–3): p. 7-14.

26. Kang, E.-T. and D.E. Day, *Oxynitride surface layers on sodium and lithium metaphosphate glasses.* Journal of Non-Crystalline Solids, 1990. **126**(1–2): p. 141-150.

27. Larson, R.W. and D.E. Day, *Preparation and characterization of lithium phosphorus oxynitride glass.* Journal of Non-Crystalline Solids, 1986. **88**(1): p. 97-113.

28. Reidmeyer, M.R. and D.E. Day, *Phosphorus oxynitride glasses.* Journal of Non-Crystalline Solids, 1995. **181**(3): p. 201-214.

29. Reidmeyer, M.R., D.E. Day, and R.K. Brow, *Phosphorus oxynitride glasses of variable sodium content.* Journal of Non-Crystalline Solids, 1994. **177**: p. 208-215.

30. Reidmeyer, M.R., M. Rajaram, and D.E. Day, *Preparation of phosphorus oxynitride glasses.* Journal of Non-Crystalline Solids, 1986. **85**(1–2): p. 186-203.

31. Achibat, T., et al., *Disorder and ramification in phosphorus oxynitride glasses.* Journal of Non-Crystalline Solids, 1992. **144**: p. 145-150.

32. Le Sauze, A. and R. Marchand, *Chemically durable nitrided phosphate glasses resulting from nitrogen/oxygen substitution within PO4 tetrahedra.* Journal of Non-Crystalline Solids, 2000. **263–264**: p. 285-292.

33. Marchand, R., *Nitrogen-containing phosphate glasses.* Journal of Non-Crystalline Solids, 1983. **56**(1): p. 173-178.

34. Munoz, F., et al., *Alkali and alkali-lead oxynitride phosphate glasses: a comparative structural study by NMR and XPS.* Comptes Rendus Chimie, 2002. **5**(11): p. 731-738.

35. Hockicko, P., P. Bury, and F. Muñoz, *Investigation of relaxation and transport processes in LiPO(N) glasses.* Journal of Non-Crystalline Solids, 2013. **363**: p. 140-146.

36. Mascaraque, N., et al., *An interpretation for the increase of ionic conductivity by nitrogen incorporation in LiPON oxynitride glasses.* Solid State Ionics, 2013. **233**: p. 73-79.

37. Mascaraque, N., et al., *Thio-oxynitride phosphate glass electrolytes prepared by mechanical milling.* Journal of Materials Research, 2015. **30**(19): p. 2940-2948.

38. Mascaraque, N., et al., *Structure and electrical properties of a new thio-phosphorus oxynitride glass electrolyte.* Journal of Non-Crystalline Solids, 2014. **405**: p. 159-162.

39. Munoz, F., et al., *Increased electrical conductivity of LiPON glasses produced by ammonolysis.* Solid State Ionics, 2008. **179**(15-16): p. 574-579.

40. Munoz, F., et al., *Conductivity study of phosphate and oxynitride phosphate glasses in the system Li2O-Na2O-PbO-P2O5.* Physics and Chemistry of Glasses-European Journal of Glass Science and Technology Part B, 2006. **47**(1): p. 58-63.

41. Paraschiv, G.L., et al., *Impact of nitridation of metaphosphate glasses on liquid fragility.* Journal of Non-Crystalline Solids, 2016. **441**: p. 22-28.

42. Riguidel, Q. and F. Munoz, *Effect of nitridation on the aqueous dissolution of Na2O-K2O-CaO-P2O5 metaphosphate glasses.* Acta Biomater, 2011. **7**(6): p. 2631-6.

43. Brinker, C.J., D.M. Haaland, and R.E. Loehman, *Oxynitride glasses prepared from gels and melts.* Journal of Non-Crystalline Solids, 1983. **56**(1–3): p. 179-184.

44. Loehman, R.E., *Preparation and properties of oxynitride glasses.* Journal of Non-Crystalline Solids, 1983. **56**(1): p. 123-134.

45. Loehman, R.E., *Oxynitride glasses.* Journal of Non-Crystalline Solids, 1980. **42**(1): p. 433-445.

46. Bates, J.B., et al., *Electrical properties of amorphous lithium electrolyte thin films.* Solid State Ionics, 1992. **53**: p. 647-654.

47. Bates, J.B., et al., *Fabrication and characterization of amorphous lithium electrolyte thin films and rechargeable thin-film batteries.* Journal of Power Sources, 1993. **43**(1): p. 103-110.

48. Wang, B., et al., *Ionic conductivities and structure of lithium phosphorus oxynitride glasses.* Journal of Non-Crystalline Solids, 1995. **183**(3): p. 297-306.

49. Yu, X., et al., *A Stable Thin-Film Lithium Electrolyte: Lithium Phosphorus Oxynitride.* Journal of The Electrochemical Society, 1997. **144**(2): p. 524-532.

50. Marchand, R., et al., *Characterization of nitrogen containing phosphate glasses by X-ray photoelectron spectroscopy.* Journal of Non-Crystalline Solids, 1988. **103**(1): p. 35-44.

51. Haaland, D.M. and C. Jeffrey Brinker, *In Situ FT-IR Studies of Oxide and Oxynitride Sol-Gel-Derived Thin Films.* MRS Proceedings, 2011. **32**.

52. Grande, T., et al., *Nitride glasses obtained by high-pressure synthesis.* Nature, 1994. **369**(6475): p. 43-45.

53. Mascaraque, N., et al., *Structure and electrical properties of a new thio-phosphorus oxynitride glass electrolyte.* Journal of Non-Crystalline Solids, 2014. **405**: p. 159-162.

54. Iio, K., et al., *Mechanochemical Synthesis of High Lithium Ion Conducting Materials in the System Li3N−SiS2.* Chemistry of Materials, 2002. **14**(6): p. 2444-2449.

55. Sakamoto, R., M. Tatsumisago, and T. Minami, *Preparation of Fast Lithium Ion Conducting Glasses in the System Li2S−SiS2−Li3N.* The Journal of Physical Chemistry B, 1999. **103**(20): p. 4029-4031.

56. Mascaraque, N., et al., *Nitrogen and fluorine anionic substitution in lithium phosphate glasses.* Solid State Ionics, 2014. **254**: p. 40-47.

57. Munoz, F., et al., *Oxidation behaviour of Li-Na-Pb-P-O-N oxynitride phosphate glasses.* Journal of the European Ceramic Society, 2006. **26**(8): p. 1455-1461.

58. Muñoz, F., et al., *Composition and structure dependence of the properties of lithium borophosphate glasses showing boron anomaly.* Journal of Non-Crystalline Solids, 2009. **355**(52-54): p. 2571-2577.

59. Fukushima, A., et al., *Mechanochemical synthesis of high lithium ion conducting solid electrolytes in a Li2S-P2S5-Li3N system.* Solid State Ionics, 2017. **304**: p. 85-89.

60. Mascaraque, N., et al., *Thio-oxynitride phosphate glass electrolytes prepared by mechanical milling.* Journal of Materials Research, 2015. **30**(19): p. 2940-2948.

61. Becher, P.F., et al., *An Overview of the Structure and Properties of Silicon-Based Oxynitride Glasses.* International Journal of Applied Glass Science, 2011. **2**(1): p. 63-83.

62. Pomeroy, M.J. and S. Hampshire, *SiAlON glasses: Effects of nitrogen on structure and properties.* Journal of the Ceramic Society of Japan, 2008. **116**(1354): p. 755-761.

63. Ahmadi, S., et al., *Preparation of monolithic oxynitride glasses by sol–gel method.* Journal of Non-Crystalline Solids, 2014. **404**: p. 61-66.

64. Krüner, G. and G.H. Frischat, *Some properties of n-containing lithium borate glasses prepared by different sol-gel methods.* Journal of Non-Crystalline Solids, 1990. **121**(1): p. 167-170.

65. Szaniawska, K., et al., *Nitridation of SiO2–B2O3 aerogels.* Journal of Non-Crystalline Solids, 2008. **354**(35-39): p. 4481-4483.

66. Kim, J.M., et al., *Li–B–O–N electrolytes for all-solid-state thin film batteries.* Journal of Power Sources, 2009. **189**(1): p. 211-216.

67. Lee, S.-J., et al., *Electrical conductivity in Li–Si–P–O–N oxynitride thin-films.* Journal of Power Sources, 2003. **123**(1): p. 61-64.

68. Mascaraque, N., et al., *Nitrogen and fluorine anionic substitution in lithium phosphate glasses.* Solid State Ionics, 2014. **254**: p. 40-47.

69. Mascaraque, N., et al., *Structural Features of LiPON Glasses Determined by 1D and 2D31P MAS NMR.* International Journal of Applied Glass Science, 2016. **7**(1): p. 69-79.

70. Paraschiv, G.L., et al., *Mixed alkali silicophosphate oxynitride glasses: Structure-property relations.* Journal of Non-Crystalline Solids, 2017. **462**: p. 51-64.

71. Anderson, O.L. and D.A. Stuart, *Calculation of Activation Energy of Ionic Conductivity in Silica Glasses by Classical Methods.* Journal of the American Ceramic Society, 1954. **37**(12): p. 573-580.

72. Martin, S.W. and C.A. Angell, *Dc and ac conductivity in wide composition range Li2O□P2O5 glasses.* Journal of Non-Crystalline Solids, 1986. **83**(1): p. 185-207.

73. Ravaine, D., *Ionic transport properties in glasses.* Journal of Non-Crystalline Solids, 1985. **73**(1): p. 287-303.

74. Martin, S.W. and D.R. Bloyer, *Preparation of High-Purity Vitreous B2S3.* Journal of the American Ceramic Society, 1990. **73**(11): p. 3481-3485.

75. Takada, K., et al., *Solid state lithium battery with oxysulfide glass.* Solid State Ionics, 1996. **86**: p. 877-882.

76. Kennedy, J.H., Z. Zhang, and H. Eckert, *Ionically conductive sulfide-based lithium glasses.* Journal of Non-Crystalline Solids, 1990. **123**(1): p. 328-338.

77. Corbridge, D.E.C. and E.J. Lowe, *The infra-red spectra of some inorganic phosphorus compounds.* Journal of the Chemical Society (Resumed), 1954(0): p. 493-502.

78. Cho, J. and S.W. Martin, *Infrared spectra of lithium thioborate glasses and polycrystals.* Journal of Non-Crystalline Solids, 1994. **170**(2): p. 182-189.

79. Kamitsos, E.I. and G.D. Chryssikos, *Borate glass structure by Raman and infrared spectroscopies.* Journal of Molecular Structure, 1991. **247**: p. 1-16.

80. Kamitsos, E.I., et al., *Infrared reflectance spectra of lithium borate glasses.* Journal of Non-Crystalline Solids, 1990. **126**(1-2): p. 52-67.

81. Geick, R., C.H. Perry, and G. Rupprecht, *Normal Modes in Hexagonal Boron Nitride.* Physical Review, 1966. **146**(2): p. 543-547.